

The Taming of the Skew: Asymmetric Inflation Risk and Monetary Policy^{*}

Andrea De Polís[†]

Leonardo Melosi[‡]

Ivan Petrella[§]

This draft: October 2025

[Click here for the latest version](#)

Abstract

We develop a tractable methodology to analyze the implications of evolving asymmetric risks in dynamic general equilibrium frameworks. Optimal policy calls for the central bank to lean against the balance of inflation risks, thereby mitigating their influence on agents' expectations. Using U.S. data, we show that inflation risks are time-varying and typically asymmetric. Using a quantitative model, we evaluate how these risks affect the macroeconomy and evaluate how a policy responding to real-time estimates of the balance of risks would have changed U.S. macroeconomic dynamics during the post-COVID rise in upside inflation risks.

Keywords: Balance of risks, optimal monetary policy, asymmetric beliefs, policy trade-offs, news and noise, risk-adjusted inflation targeting, geopolitical risks.

JEL codes: E52, E31, C53.

^{*}We would like to thank Guido Ascari, Gianluca Benigno, Domenico Giannone, Emmanuel Moench, Roberto Motto, Matthias Rottner, and the seminar participants at the Federal Reserve Bank of Chicago, the Federal Reserve Bank of Cleveland, the De Nederlandsche Bank, the University of Lausanne, the Workshop on the Economics of Risk Econometric Tools and Policy Implications at Collegio Carlo Alberto, Turin, the workshop on Monitoring and Forecasting Macroeconomic and Financial Risk at the National Central Bank of Belgium, the 2nd Annual Non-Linearities in Macro Workshop at the Bank of England, the Workshop on Empirical Monetary Economics at OFCE Paris, and the Inflation: Drivers and Dynamics 2025 Conference at the ECB. Leonardo Melosi is grateful to the European Central Bank for its generous hospitality and support during the summer of 2024, where a significant portion of this work was conducted. Any views expressed in this paper are those of the authors and do not necessarily reflect the views of Banco de España or any other person associated with the Eurosystem.

[†]Banco de España. andrea.depolis@bde.es

[‡]European University Institute & CEPR. leonardo.melosi@eui.eu

[§]Collegio Carlo Alberto, University of Turin & CEPR. ivan.petrella@carloalberto.org

The pandemic and war have underscored the need for the risk management framework to take full account of both upside and downside risks to inflation, as well as to the possibility that serious tensions may arise between the objectives of price stability and employment or growth.

Gita Gopinath, Jackson Hole Symposium, August 26, 2022

1 Introduction

Since the pandemic, the global economy has been increasingly facing rising geopolitical tensions and fragmentation, amplifying macroeconomic risks and raising the likelihood of future inflation surges and deep recessions. This new environment marks a clear departure from the pre-pandemic era, when macroeconomic risks were relatively subdued and inflation consistently surprised on the downside. Scholars and policymakers are debating whether the shifting balance of risks gives rise to novel challenges for macroeconomic stabilization and new policy trade-offs, as exemplified by Gita Gopinath, First Deputy Managing Director of the International Monetary Fund, in the opening quotation.

In this paper, we develop a tractable methodology to investigate how shifts in the balance of macroeconomic risks affect the macroeconomy and to characterize the central bank’s optimal response. The model features cost-push shocks drawn from a distribution with time-varying skewness. Agents receive news about changes in the skewness of the distribution, shaping their perception of macroeconomic risks. These evolving perceptions create time-varying asymmetries in agents’ beliefs, which, in turn, affect equilibrium outcomes and introduce an additional trade-off for the central bank.

As standard since the seminal contributions of [Clarida et al. \(1999\)](#); [Woodford \(2003\)](#), we study optimal monetary policy in a linear-quadratic approximation of our model. While symmetric changes in risk have no first-order impact on equilibrium outcomes, asymmetric ones do, as they shift agents’ expectations. In a linear model, expectations are the only relevant moment of beliefs, so changes in skewness directly affect decisions by tilting the mean toward one tail of the distribution. One advantage of the linear-quadratic approach is to allow an analytical characterization of optimal monetary policy in the model and a direct comparison with optimal monetary policy under symmetric shocks.

We find that optimal monetary policy requires central banks to actively counteract *inflation risks* arising from asymmetric cost-push shocks. This approach reflects the need to counter the deanchoring of inflation expectations from the central bank’s target induced by the asymmetric distribution of shocks. When positive cost-push shocks are expected to become more likely, inflation expectations tend to rise above the central bank’s target. In response, the optimal policy involves a preemptive tightening to anchor expectations and contain inflation risks. Conversely, when the likelihood of negative cost-push shocks increases, the central bank should ease monetary policy to stimulate aggregate demand and raise inflation expectations, thereby offsetting the disinflationary effects.

For this normative prediction to be relevant in practice, there must be sufficient evidence that shifts in the balance of inflation risks are a significant feature of the data and that changes in risk asymmetry can be reliably tracked in real-time. Using data on U.S. core Personal Consumption Expenditure (PCE) inflation, we find robust evidence supporting time-varying asymmetry in the predictive distribution of inflation. Specifically, we propose a model capable of estimating and predicting the evolving asymmetry in inflation risks in real-time. Our analysis identifies statistically significant and frequent shifts in the balance of inflation risks throughout the postwar period, often following persistent, regime-like patterns. We validate the model by showing that incorporating time-varying skewness into inflation forecasts significantly enhances out-of-sample accuracy compared to standard benchmark models ([Stock and Watson, 2007](#)), achieving predictive performance on par with the *Survey of Professional Forecasters* (SPF).

We then leverage the tractability of our linear approach to solve a quantitative structural model that replicates the balance of inflation risks estimated in real-time. Specifically, we construct a sequence of news shocks such that the impact of skewness on agents’ inflation expectations in the structural model matches the corresponding effect estimated from real-time data. We then use this structural model in two ways. First, we quantify the macroeconomic effects of shifts in the balance of inflation risks driven by changes in the asymmetry of cost-push shocks. We find that an increase in inflation asymmetry, corresponding to upside risk 25% higher than downside risk, leads to up to 1% percentage point rise in inflation and 2% percentage point decline in hours worked.

Second, we define a novel monetary policy strategy—the Risk-Adjusted Inflation Targeting (RAIT)—and produce counterfactual scenarios under this policy. The RAIT calls for the central bank to dynamically adjust its communication about the future path of the policy rate to counter shifts in the balance of inflation risks. In the model, these adjustments are designed to completely shelter inflation expectations from distortions caused by asymmetric inflation risks. As a result, the RAIT ensures, by construction, that inflation expectations remain stable and anchored at the central bank’s target in every period.

We compare the counterfactual dynamics of key macroeconomic variables under the RAIT to those observed in the data. During the recent inflation surge, real-time estimates indicate that inflation risks became heavily tilted to the upside. Under these conditions, the RAIT would have recommended an earlier liftoff in interest rates, reaching a peak similar to that observed in the data but slightly sooner. By early 2023, the RAIT would have called for a faster unwinding of the prior monetary tightening. The model predicts that, under the RAIT, inflation would have declined more quickly, reaching the Federal Reserve’s target by early 2023 and stabilizing thereafter. By initiating monetary easing in early 2023, the RAIT would have also supported the labor market, partially offsetting the effects of the earlier tightening.

The RAIT offers a forward-looking, risk-based alternative to the “Flexible Average Inflation Targeting” (FAIT) framework adopted by the Federal Reserve in 2020 in response to persistent deflationary risks (Clarida, 2022). While FAIT bases overshooting on past deviations from the 2% target, the RAIT adjusts policy in response to real-time assessments of changes in balance of inflation risks. This dynamic, model-based approach makes the RAIT more responsive to sudden shifts in skewness, such as those seen in the post-Pandemic period.

Literature Review This paper contributes to the relatively limited literature on risk management in monetary policy. Previous work by Dolado et al. (2004) and Surico (2007) shows that asymmetric preferences can justify nonlinear policy rules. Kilian and Manganelli (2008) stress the need to balance upside and downside risks under asymmetric loss functions.¹ In these settings, central banks may optimally target average inflation above or below the policy target when the

¹Kilian and Manganelli (2007) measure inflation risks under time-varying symmetric volatility.

costs of deviations are asymmetric—a bias that vanishes under symmetric preferences. Our key contribution is to show that when inflation risk is asymmetric, optimal policy must still account for the balance of risks, even with a symmetric target. Importantly, we highlight that shifts in skewness create a gap between the modal forecast and expected inflation. This divergence has macroeconomic effects, and neglecting it leads to systematic deviations from target over time.

[Evans et al. \(2020\)](#) show that uncertainty around the ZLB calls for looser monetary policy and a delayed liftoff, and provide evidence that the Federal Reserve frequently incorporates risk management in setting rates. [Bianchi et al. \(2021\)](#) argue that an asymmetric policy strategy can offset the deflationary bias from the risk of repeatedly hitting the ZLB. Unlike these studies, we focus on how central banks should respond to broader shifts in the balance of macroeconomic risks—not limited to the ZLB. Our contribution is to show how time-varying asymmetric risks can be embedded within a structural model, allowing for the explicit analysis of monetary strategies that target inflation risks directly.

This paper contributes to the literature on optimal inflation targeting ([Giannoni and Woodford, 2004](#)) by examining the empirical effects of strategies like the RAIT. By ensuring that the central bank’s mean inflation forecasts align with its policy objectives, the RAIT falls within the broader category of strategies studied by [Svensson \(1997\)](#), commonly known as forecast inflation targeting. Our main innovation is to formulate the optimal policy problem in an environment where the balance of macroeconomic risks evolves stochastically.² Unlike most of the forecast targeting literature, which often limits policy to reacting to current or lagged variables, our approach allows the central bank to respond to forward-looking endogenous variables—capturing the dynamic interaction between policy, expectations, and evolving risk perceptions.

Our work also connects to the growing literature highlighting the role of news, sentiment, and noise shocks in driving macroeconomic dynamics (see, e.g., [Angeletos and La’o, 2010](#); [Chahrour and Jurado, 2018](#)). We show that the first-order effects of changes in risk asymmetry can be equivalently represented as sentiment or pure noise shocks, altering expectations without necessarily

²[Svensson \(2003\)](#) discusses how central banks should implement their reaction functions in the presence of unbalanced macroeconomic risks, reviewing and critiquing practices such as the Bank of England’s choice to display the mode rather than the mean in fan charts for output and inflation. These critiques have been recently echoed by [Bernanke \(2024\)](#).

materializing. Focusing on cost-push shocks, we emphasize how belief-driven distortions shape inflation expectations and matter for the design of optimal monetary policy.

Our paper also contributes to the literature on inflation forecasting, which has largely focused on slow-moving trends and time-varying uncertainty (see, e.g., [Cogley and Sargent, 2005](#); [Stock and Watson, 2007](#); [Faust and Wright, 2013](#); [Ascari and Sbordone, 2014](#)). Far less attention has been paid to asymmetries in inflation risk. Notable exceptions include [Andrade et al. \(2014\)](#), [Mouabbi et al. \(2025\)](#) and [Hilscher et al. \(2022\)](#), who use survey and options data to assess tail risks. In contrast, we develop an econometric model for the full predictive density of U.S. core PCE inflation that explicitly accounts for asymmetry via a Skew-t distribution (see [Arellano-Valle et al., 2005](#)). Our framework adopts the score-driven approach of [Harvey \(2013\)](#) and [Creal et al. \(2013\)](#), as in [Delle Monache et al. \(2024\)](#), to allow time variation moments of inflation. This sets our work apart from other full-density inflation forecasting models (e.g., [Manzan and Zerom, 2013, 2015](#); [Korobilis et al., 2021](#); [Le Bihan et al., 2024](#)), which mainly rely on quantile regressions and assume risk evolves linearly with known predictors. Notably, [López-Salido and Loria \(2024\)](#) document variability in the tails of inflation linked to financial and macroeconomic conditions. These studies, however, focus on shorter time periods, often omitting the high-inflation episode of the 1970s, and do not relate asymmetric inflation risks to macroeconomic dynamics and optimal policy within a structural DSGE framework.

Structure The remainder of the paper is organized as follows. [Section 2](#) explains how shifts in risk affect macroeconomic allocations in a general DSGE framework and introduces the beliefs representation of a model with asymmetric risks. In [Section 3](#), we characterize optimal monetary policy within a New Keynesian model featuring asymmetric macroeconomic risks. [Section 4](#) provides empirical evidence on the relevance of inflation skewness in the U.S. In [Section 5](#), we calibrate the beliefs representation of a quantitative DSGE model to match the estimated balance of risks from the econometric model and conduct policy counterfactuals. [Section 6](#) concludes.

2 Theoretical Framework

In this section, we highlight how shifts in the asymmetry of future macroeconomic risks influence equilibrium outcomes within a linear general equilibrium framework. We prove that changes in the perception of asymmetric risk can be interpreted as revisions in agents' beliefs about the future distribution of shocks. The complete proof of this result, along with supporting claims, is provided in [Appendix A](#). In this section, we prove two propositions showing that a linearized model in which agents receive signals about the likely evolution of the skewness of the shock distribution can be recast as a linear rational expectations model with news shocks. As a result, it can be solved using standard methods.

The set of models to which our methodology can be applied is very broad. We impose only two core assumptions. First, agents are assumed to expect the distribution of shocks to be symmetric in the long run, so there is no need to account for a risky steady state. Consequently, the only relevant steady state around which the model is log-linearized is the deterministic (or non-risky) one, which remains unaffected by short-term fluctuations in the skewness of the shock distribution. Second, for ease of exposition, we focus on the family of two-piece distributions, introduced by [Fechner \(1897\)](#), which includes a large set of univariate skewed distributions (see, e.g., [Fernández and Steel, 1998](#); [Arellano-Valle et al., 2005](#)). These distributions are flexible and convenient, making them widely used in finance, econometrics, and various other fields such as environmental and ecology studies and engineering, for modeling asymmetric risks surrounding future events.

2.1 Shifting asymmetries in linear general equilibrium models

Linearized rational expectations general equilibrium models, widely used in theoretical and empirical macroeconomic research, can be expressed as follows:

$$\mathbf{A}_0 \mathbf{z}_t = \mathbf{A}_f E_t \mathbf{z}_{t+1} + \mathbf{A}_b \mathbf{z}_{t-1} + \mathbf{B}_s \boldsymbol{\epsilon}_t^s + \mathbf{b}_a \boldsymbol{\epsilon}_t^a. \quad (1)$$

where \mathbf{z}_t collect endogenous and exogenous variables, the operator E_t denotes rational expectations conditional on the information set available at time t , which, as we will describe, contains the

history of all the shocks. The vectors of i.i.d. disturbances are denoted by ϵ_t^s and ϵ_t^a . The former includes all the symmetric shocks, e.g., normally distributed, whereas the latter is a possibly *asymmetric* shock with distribution $f(\mu_a, \sigma_a, \varrho_a)$, where μ_a denotes the mode, σ_a the scale, and ϱ_a an asymmetry parameter that measures the degree of skewness.³ Without loss of generality, the mode μ_a can be set to zero, as it can be absorbed into the definition of the steady state.⁴

For $\varrho_a > 0$ ($\varrho_a < 0$), f is positively (negatively) skewed, while $\varrho_a = 0$ implies symmetry. Asymmetric risk implies that the probability mass around the mode is unevenly distributed: risks are skewed to the downside (upside) when outcomes below (above) μ are more likely than those above (below) it.⁵ In [Appendix A.1](#), we derive the log-linear system in [Equation \(1\)](#) as a first-order Taylor expansion around the steady state of the full nonlinear model with skewed shocks.

Time-varying asymmetric risk. In the class of two-piece distributions, the wedge between the expected value, Ef , and the mode μ_a (the *mean-mode wedge*, for short), depends on the linear mapping $Ef = \mu_a + \varkappa \sigma_a \varrho_a$, with $\varkappa > 0$. The exact definition of \varkappa depends on the specific functional form of the skewed distribution.⁶

A distinctive feature of our analysis is the assumption that the asymmetry parameter of the distribution f , denoted $\varrho_{a,t}$, varies over time. This means the economy can shift between periods of upside and downside risk, with the severity of each episode changing over time. We assume that the asymmetry parameter follows a stationary zero-mean process; i.e., $E(\varrho_{a,t}) = 0$. The other parameters, mode and scale are held constant, with the mode set to zero without loss of generality. These restrictions can be relaxed, but are maintained in the interest of analytical tractability.⁷

³While we focus on the case with a single source of asymmetric risk, extending the analysis to multiple independent asymmetric shocks is straightforward and does not alter the underlying intuition.

⁴Recall that the distribution of shocks, ϵ_t^a , is expected to become symmetric in the long run. As a result, the long-run mean and mode of ϵ_t^a coincide.

⁵Let $r = \int_{\mu}^{\infty} f dx / \int_{-\infty}^{\mu} f dx$ be the ratio of probability mass right and left of the mode. Then, $\varrho = \frac{r-1}{r+1} \in (-1, 1)$.

⁶For a Skewed-Normal distribution, $\varkappa = \sqrt{2/\pi}$. For the Skewed- t distribution—used later in the paper— \varkappa depends on the degrees of freedom (see, e.g., [Arellano-Valle et al., 2005](#)). Intuitively, when the distribution has fat (thin) tails, the effect of skewed risk on expected outcomes becomes larger (smaller).

⁷Introducing stochastic variation of the mode would not alter any results of this Section, provided that these changes do not completely offset the effects of skewness on the expected value of the shocks. In the empirical analysis, we will jointly estimate the evolution of the three parameters of the predictive distribution of inflation.

Agents beliefs. Agents are rational and perfectly informed. They know the parameters in Equation (1), the history of the realized shocks, and the shocks distributions, including the mode μ , the scale σ , the past and current realizations of the asymmetry of f .

Agents receive news about the future evolution of the distribution's asymmetry, $\varrho_{a,t}$, which is the stochastic parameter driving the mean-mode ($Ef - \mu_a$). In every period t , agents receive a set of noisy signals about the future evolution of the asymmetry parameter over the next $J > 0$ periods. At every horizon $j \in \{1, \dots, J\}$ agents observe the signal $s_t^j = \varrho_{a,t+j} + \eta_t^j$, where η_t^j denote the zero-mean noise orthogonal to the future realizations of the asymmetric parameter.

Rational agents solve the signal extraction problem, updating expectations about the asymmetry parameter j periods ahead. We denote these iid updates as $\varrho_{a,t}^j \equiv E_t \varrho_{a,t+j} - E_{t-1} \varrho_{a,t+j}$.

Model dynamics, forecasts, and central scenarios. As a consequence of the certainty equivalence in a linear setting, only expectations matter for the first-order solution of the model.

Proposition 1. *The solution of the linear rational expectations model with time-varying skewness in Equation (1) reads:*

$$\mathbf{z}_t = \Theta_1 \mathbf{z}_{t-1} + \Theta_0 [\epsilon_t^s \epsilon_t^a]' + \Theta_y \sum_{j=1}^{\infty} \Theta_f^{j-1} \Theta_z \Xi E_t \epsilon_{t+j}^a, \quad (2)$$

where Ξ is a selection vector, and the matrices Θ_0 , Θ_1 , Θ_y , and Θ_z are functions of \mathbf{A}_0 , \mathbf{A}_b , \mathbf{A}_f , \mathbf{B}_s , and \mathbf{b}_a .

Proof. See Appendix A.2. □

Proposition 1 establishes that anticipated changes in the asymmetry parameter of future shock distributions, $\varrho_{a,t+j}$, affect equilibrium outcomes as they lead agents to revise their expectations about the future realizations of the shocks $E_t \epsilon_{t+j}^a$.

While the first two terms on the right-hand side of Equation (2) are standard, the third term captures the role of agents' beliefs about the evolution of asymmetry, which depend on the noisy signals agents receive. If the signals are not informative of the asymmetry of future shocks ϵ_{t+j}^a , or if the news leads to the belief that shocks will be symmetric ($E_t \varrho_{t+j} = 0, \forall j$), the expected value

of future asymmetric shocks is zero. As a consequence, the third term on the right-hand side of Equation (2) drops out, and the solution simplifies to the familiar form: $\mathbf{z}_t = \Theta_1 \mathbf{z}_{t-1} + \Theta_0 [\epsilon_t^s \epsilon_t^a]'$.

Proposition 1 highlights that, when agents expect asymmetric shocks over the forecast horizon, the expected outcomes diverge from the modal forecast, $\mathbf{z}_{t+j} = \Theta_1^j \mathbf{z}_t$, due to the influence of risk perceptions on agents' expectations.

First-order effects of expected changes in asymmetry. An important implication of modeling asymmetric shocks using a two-piece distribution is that expected changes in the asymmetry parameter of j -period-ahead shocks, $E_t \varrho_{a,t+j}$, affect equilibrium outcomes *only* through their impact on the expected value of future shocks, $E_t \epsilon_{t+j}^a$. Specifically, these effects on expectations are given by

$$E_t \epsilon_{t+j}^a = \varkappa \sigma_a E_t \varrho_{a,t+j}. \quad (3)$$

The model solution in Equation (2), together with Equation (3), makes clear how changes in the expected asymmetry of future risks influence macroeconomic dynamics.

Revisions in the asymmetry parameter lead to revisions in expectations about future shocks, i.e., $E_t \epsilon_{t+j}^a - E_{t-1} \epsilon_{t+j}^a = \varkappa \sigma_a \varrho_{a,t}^j$. Thus, even though the most likely outcome (the mode) remains unchanged, a shift in the balance of risks prompts an immediate adjustment in current equilibrium allocations and expectations:

$$E_t \mathbf{z}_{t+h} - E_{t-1} \mathbf{z}_{t+h} = \mathbf{M}(j, h) \varkappa \sigma_a \varrho_{a,t}^j, \quad h \geq 0, \quad (4)$$

where $\mathbf{M}(j, h)$ is a convolution of the system matrices in Equation (2).

2.2 Beliefs representation

We now show that, to a first-order approximation, a model with asymmetric risks can be equivalently represented as one with symmetric, zero-mean shocks, augmented by additional *beliefs* shocks. These belief shocks capture revisions to agents' expectations following the arrival of the signals. We refer to this formulation as the model's *beliefs representation*. The key advantage of

this representation is that it can be solved using off-the-shelf, standardized solution techniques.

This representation preserves the linearized equilibrium laws of motion that characterize the dynamics of the original model with asymmetric risks. The only point of departure is the introduction of *dummy surprise and anticipated shocks* that encode belief-driven distortions.

In the beliefs representation, we define the realizations of asymmetric shock as the sum of past news shocks and current shock:

$$\epsilon_t^a \equiv \sum_{j=0}^J \varphi_{a,t-j}^j, \quad (5)$$

where φ_t^j denotes the dummy beliefs shocks.

The following proposition provides the restrictions on the stochastic process of the dummy beliefs shocks ensuring that the beliefs representation is equivalent to the actual model with time-varying asymmetry.

Proposition 2. *The equilibrium dynamics of the beliefs representation are identical to the ones of the actual economy—shown in Equation (2)—if the following two conditions hold: (i) The dummy anticipated shocks $\varphi_{a,t}^j$ match the revisions in expectations regarding the asymmetry of the distribution of future shocks at each horizon:*

$$\begin{aligned} \varphi_t^j &= E_t \epsilon_{a,t+j} - E_{t-1} \epsilon_{a,t+j} \\ &= \kappa \sigma_a (E_t \varrho_{a,t+j} - E_{t-1} \varrho_{a,t+j}) \\ &= \kappa \sigma_a \varrho_{a,t}^j, \quad \forall j \in 1, \dots, J, \end{aligned} \quad (6)$$

where $\varrho_{a,t}^j$ denotes agents' revision about expected risk asymmetry after observing the signal, s_t^j , in the actual model. (ii) The surprise dummy shock must satisfy the following condition

$$\varphi_t^0 = \epsilon_{a,t} - \sum_{j=1}^J \varphi_{t-j}^j, \quad \forall t. \quad (7)$$

Proof. As per Equation (3), changes in the expected evolution of the asymmetry affect equilibrium outcomes only through their impact on expectations about future shocks. Condition (i) ensures that the dummy belief shocks replicate the same impact of anticipated asymmetry on the

expectations $E_t \epsilon_{a,t+j}$. Condition (ii) ensures that, in every period, the realization of the shock $\epsilon_{a,t}$ exactly matches that in the actual economy. These two conditions guarantee that the beliefs representation replicates the structure of the actual economy, the realizations of shocks, and agents' expectations about future realizations of asymmetric shocks. As a result, its equilibrium outcomes satisfy Equation (2) in Proposition 1. Detailed derivations are available in Appendix A.4. \square

Proposition 2 establishes the key result that the beliefs representation is isomorphic to an economy in which agents receive news regarding the evolving balance of risks. Hence, owing to its tractability, solving the belief representation allows to easily derive the equilibrium laws of motion of the actual economy in Equation (2). It is worth noting that standard solution techniques for linear rational expectations remains effective even when the signal extraction problem may lead to non-Gaussian revisions to expectations of future shocks. These solvers typically do not restrict the stochastic process of the shocks beyond the iid and mean zero assumptions, which are not restrictive in most cases.

In the belief representation, shocks are related to revisions in expectations about the asymmetry of future shock, as shown in Equation (6). Hence, these shocks are iid, in line with rational expectations models, where revisions to expectations about future shocks are unpredictable.

The beliefs representation can be used to study environments where agents receive news about future risks, conveyed through changes in the scale and asymmetry of future shock distributions. To a first-order approximation, anticipated changes in either parameter affect allocations by shifting the expected value of future shocks—thus preserving the relevance of the beliefs-based approach.

As shown in Equation (3), the effect of the asymmetry depends on the scale of the distribution: a shift in skewness has a larger impact on expectations when uncertainty is high (i.e., when σ_a is large). Likewise, when distributions are skewed, changes in uncertainty influence mean outcomes, even when asymmetry is unchanged. The direction and magnitude of these effect depend on the sign of the skew. In the next sections, we apply this framework to analyze how shifts in perceived risk should inform the conduct of monetary policy.

3 Optimal monetary policy with asymmetric risks

In this section, we examine the implications of time-varying asymmetric macroeconomic risk for optimal monetary policy within the textbook New Keynesian model with sticky prices. We first review optimal policy in a linear-quadratic framework under symmetric risk, as presented in Galí (2008, Chapter 3 and 5). We then extend the analysis to account for shifts in asymmetric risk, using the tools developed in the previous section. Detailed derivations are provided in Appendix B.

3.1 The case of symmetric risks

Let us assume that the central bank can fully commit, with credibility, to a policy plan by selecting a state-contingent sequence of inflation deviations from its target and output gaps, $\{\hat{\pi}_t, \hat{x}_t\}_{t=0}^{\infty}$, to minimize the loss function $-\frac{1}{2}E_0 \sum_{t=0}^{\infty} \beta^t (\hat{\pi}_t^2 + \alpha_x \hat{x}_t^2)$, subject to the sequence of constraints given by the Phillips curve, $\hat{\pi}_t = \beta E_t \pi_{t+1} + \kappa \hat{x}_t + u_t$. We further assume that the cost-push shock follows $u_t \sim iid \mathcal{N}(0, \sigma_u)$, implying symmetric risks.⁸

Under the optimal policy, the central bank sets the output gap proportional to the deviations of the price level from its implicit target: $\hat{x}_t = -\frac{\kappa}{\alpha_x} \bar{p}_t$, where $\bar{p}_t = p_t - p_{-1}$ denotes the cumulative inflation rate from the period preceding the implementation of optimal plan. This condition can be interpreted as a targeting rule that the central bank is required to follow in every period in order to implement the optimal policy.

Under optimal policy, the price level evolves according to

$$\bar{p}_t = \eta \bar{p}_{t-1} + \lambda u_t, \quad (8)$$

and the corresponding optimal monetary policy rule is given by

$$\hat{i}_t = -(1 - \eta) \left[1 - \sigma \frac{\kappa}{\alpha_x} \right] \bar{p}_t, \quad (9)$$

⁸All variables are expressed in log-deviations from their steady-state value. The objective function is the quadratic approximation of the household's utility function, with weight on the output gap $\alpha_x = \kappa/\varepsilon$, where ε denotes the elasticity of substitution and κ is the slope of the Phillips curve.

where σ is the inverse of the household's intertemporal elasticity of substitution, and η and λ are functions of the structural parameters of the model.

3.2 The case of asymmetric risks

Let us now consider the case where the stochastic process driving the cost-push shock is no longer symmetric. Assume that the shock follows $\tilde{u}_t \sim iid f(0, \sigma_u, \varrho_{u,t})$, where $f(0, \sigma_u, \varrho_{u,t})$ denotes a general two-piece distribution centered at zero. The asymmetry of the distribution evolves over time, as agents update their views about the balance of risks, driven by $\varrho_{u,t} \neq 0$. As a result, the expected value of future shocks reflects changes in perceived asymmetry. While the mode—the most likely outcome—remains at zero, the mean shifts with asymmetry: $E_t \tilde{u}_{t+j} = \varkappa \sigma_u E_t \varrho_{u,t+j}$.

To simplify the characterization of optimal monetary policy, we assume that agents receive news about the skewness of the distribution only up to $J = 1$ period ahead. Beyond that, they assume risk to be symmetric. At time t , agents observe the current realization and form expectations about future realizations of the shocks, based on their current perception of the skewness of risk. This implies $E_t \tilde{u}_{t+1} = \varkappa \sigma_u E_t \varrho_{u,t+1}$, while $E_t \tilde{u}_{t+j} = 0, \forall j > 1$. Moreover, since $\varrho_{u,t+1} = \varrho_{u,t+1}^0 + \varrho_{u,t}^1$, and assuming agents do not anticipate further revisions in asymmetry (i.e., $E_t \varrho_{u,t+1}^0 = 0$), it follows that $E_t \tilde{u}_{t+1} = \varkappa \sigma_u \varrho_{u,t}^1$, where $\varrho_{u,t}^1 = E_t \varrho_{u,t+1} - E_{t-1} \varrho_{u,t+1}$. Expectations of future shocks therefore reflect the latest update in perceived risk asymmetry.

As discussed in [Section 2.2](#), up to a first-order approximation, the dynamics of a model with evolving perceptions of asymmetric risk can be equivalently represented by a model with symmetric shocks and belief distortions captured by dummy surprises. Specifically, we introduce a tilt in agents' beliefs, $E_t(\tilde{u}_{t+1}) = \varphi_{t,t+1}$, with beliefs evolving over time according to $\varphi_{t,t+1} = \varphi_t^0 + \varphi_{t-1}^1$. Setting $\varphi_t^1 = \varkappa \sigma_u \varrho_{u,t}^1$, and imposing the restriction $\varphi_t^0 = -\varphi_{t-1}^1$, ensures that belief revisions replicate the impact of changes in perceived asymmetry on the expected value of the shock, while leaving the actual realization unaffected.

The optimal policy retains the form: $\hat{x}_t = -\frac{\kappa}{\alpha_x} \bar{p}_t$ but both the price level and the output gap are now influenced by shifts in risk. Specifically, their equilibrium dynamics under this policy can

be characterized analytically as follows:

$$\bar{p}_t = \eta \bar{p}_{t-1} + \lambda u_t + \zeta \varphi_t^1. \quad (10)$$

Macroeconomic risks create a wedge between agents' expectations and the modal scenario—that is, the expectations they would hold under symmetric risk. As a result, positive (negative) shifts in the balance of risk lead to upward (downward) movements in prices, as firms incorporate upside (downside) risks to future costs into current pricing decisions (since $\varphi_t^1 \propto \varrho_{u,t}^1$).⁹

The optimal policy requires the central bank to respond to the effects of the changing balance of macroeconomic risks on agents' expectations:

$$\hat{i}_t = -(1 - \eta) \left[1 - \sigma \frac{\kappa}{\alpha_x} \right] \bar{p}_t + \left[1 - \sigma \frac{\kappa}{\alpha_x} \right] \lambda \varphi_t^1. \quad (11)$$

The first term represents the optimal rule under symmetry, while the second captures the policy rate adjustment required to offset the effects of the balance of risks on agents' expectations.

3.3 The case of asymmetric risks with an unwitting central bank

Assume now that the central bank chooses its optimal policy without internalizing that macroeconomic risks are symmetric, whereas agents are aware of it. As we will show, this scenario makes an useful counterfactual scenario to draw intuition regarding the key features of the optimal policy under asymmetric shocks.

In this case, the central bank sets the output gap to achieve a price level consistent with the assumption that shocks are symmetrically distributed: $\hat{x}_t = -(\kappa/\alpha_x) \bar{p}_t^m$, where $\bar{p}_t^m = p_t^m - p_{-1}$ and p_t^m is the price level the central bank believes it could achieve with its policy under the incorrect assumption of symmetric risks. This (unattainable) price level is defined as: $\bar{p}_t^m = \eta \bar{p}_{t-1} + \lambda u_t$, where \bar{p}_{t-1} is the previous period's equilibrium price level. Note that the anticipated dummy shock, φ_t^1 , which captures the tilting of the private sector's expectations about the price level today, does

⁹The output gap moves in the opposite direction, reflecting the trade-off induced by cost-push shocks: $\hat{x}_t = \eta \hat{x}_{t-1} - \frac{\kappa}{\alpha_x} [\lambda u_t + \zeta \varphi_t^1]$.

not appear in the equation, as the central bank overlooks the effects of asymmetric risk. As a result, the output gap will be suboptimal and under an equilibrium price level that is different from p_t^m sought by the central bank. Detailed derivations are provided in Appendix [Appendix B](#).

3.4 A illustrative example

We now illustrate the role of optimal monetary policy in the presence of asymmetric risks.¹⁰ Assume the economy is initially at its steady state. In period $t = 0$, agents receive news that the distribution of cost-push shocks in period $t = 1$ will be positively skewed. This upside risk is captured by a dummy anticipated shock $\varphi_0^1 = 0.8$. In period $t = 1$, a positive cost-push shock materializes, with $\varepsilon_1^u = 0.8$, while all other periods feature symmetric shocks with zero mean. The path of the cost-push shock and the evolution of agents' expectations, represented by φ_t^1 , are shown in the bottom-right panel of [Figure 1](#).

The remaining panels display the responses of the output gap, interest rate, and price level. The black solid line represents the benchmark with symmetric risks ($\varphi_t^1 = 0$), where the economy responds only to the realized cost-push shock at $t + 1$. This results in higher inflation, a negative output gap, and a persistent rise in interest rates to restore price stability. The blue line shows the case where agents anticipate upside risk at $t = 0$. When future cost-push shocks are expected to be skewed upward, firms incorporate those into current pricing, raising inflation. A central bank that internalizes this risk tightens policy preemptively, leading to lower demand and a negative output gap already at $t = 0$.

The unwitting central bank chooses the same output gap as in the symmetric case (the black solid line) because it aims to achieve the same price level. However, agents' expectations are distorted by the negative skewness in the distribution of cost-push shocks for the next period. As a result, the desired price level turns out to be unattainable, with the equilibrium price level being higher in period zero. This is reflected in the red dashed-dotted line jumping above the black solid line at time 0 in the bottom-left panel.¹¹

In summary, when risks are skewed, optimal policy must lean against the direction of asymme-

¹⁰Model parameters follow [Gali \(2008, Chapter 3\)](#) and are reported in [Appendix B](#).

¹¹The desired output gap under symmetric shocks is zero, as no shocks hit the economy in period 1.

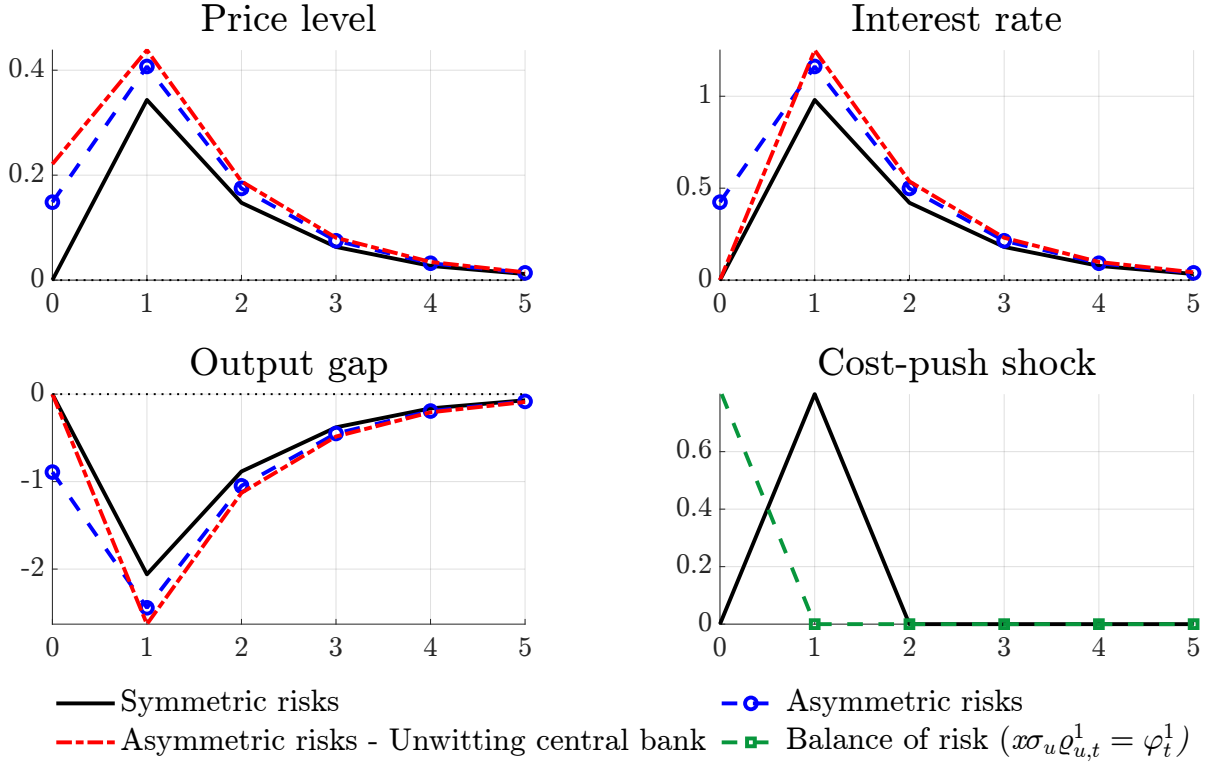


Figure 1: Optimal monetary policy under symmetric and asymmetric macroeconomic risks.

Note: The panels report the macroeconomic effects of a cost-push shocks drawn from a symmetric distribution (black) and from an asymmetric distribution (blue) under optimal monetary policy. The red line denotes a counterfactual case where risks are asymmetric but the central bank does not take that into account and targets an unattainable price level \bar{p}_t^s (red stars). The lower right panel shows the cost-push shock, u_t (black), which hits the economy in period $t+1$, as well as the anticipated skewness (φ_t^1), in green.

try. Positive skewness in inflation risk calls for a policy stance that reduces inflation expectations and tolerates an output contraction. If risks were skewed to the downside, the central bank would instead overheat the economy. More generally, symmetric risk delivers higher welfare, highlighting the challenges that asymmetric risks pose for monetary policy.

4 An econometric framework for inflation risk

Having established that changes in the balance of inflation risks warrant a policy response, the practical relevance of this insight rests on the central bank's ability to monitor these risks over time. We introduce a time series model to estimate time-varying predictive densities of inflation in real-time. Building on standard unobserved components frameworks (see, e.g., [Stock and Watson, 2007](#)), the model incorporates time-varying skewness in the inflation distribution. We show that

considering changes in the asymmetry of risk improves out-of-sample forecast accuracy, highlighting the value of higher-order moments in understanding and predicting inflation risks. The model is estimated using quarterly data on US core PCE inflation, from 1960Q1 to 2024Q4.

4.1 Model specification

Let $\pi_t = 400 \log(p_t/p_{t-1})$ denote the annualized, quarter-on-quarter (core) PCE inflation rate, and assume that at each point in time the distribution of π_t can be characterized by a Skew-t (Sk_t) distribution with time-varying location (μ_t), scale (σ_t), and shape (ϱ_t) parameters:

$$\pi_t \sim Skt_\nu(\mu_t, \sigma_t^2, \varrho_t), \quad (12)$$

where ν denotes the, time invariant, degrees of freedom. The degree of the asymmetry is risk is captured by the parameter $\varrho_t \in (-1, 1)$. The distribution of inflation realizations is positively (negatively) skewed for $\varrho_t > 0$ ($\varrho_t < 0$) and the underlying right- and left-risk around the central scenario (mode), μ_t , can be retrieved as $\sigma_t(1 - \varrho_t)$ and $\sigma_t(1 + \varrho_t)$. This specification allows as special cases: (i) the symmetric Student-t distribution when $\varrho_t = 0$, (ii) the epsilon-Skew-Gaussian for $\nu \rightarrow \infty$, and (iii) the Gaussian density when both conditions hold jointly. Thus, we allow for, but do not impose, asymmetric innovation terms.

Following a long tradition in modeling the stochastic properties of inflation (see e.g., [Cogley, 2002](#); [Stock and Watson, 2007](#); [Faust and Wright, 2013](#)), we treat the time-varying parameters as unobserved components that can be learned in real-time. Specifically, let $\delta_t = \log(\sigma_t)$ and $\gamma_t = \text{arctanh}(\varrho_t)$, we postulate that each element $f_{i,t}$ of $f_t = (\mu_t, \delta_t, \gamma_t)'$ features a permanent and transitory component: $f_{i,t} = \bar{f}_{i,t} + \tilde{f}_{i,t}$, which evolve as¹²

$$\bar{f}_{i,t} = \bar{f}_{i,t-1} + a_i s_{i,t-1}, \quad (13)$$

$$\tilde{f}_{i,t} = \phi_i \tilde{f}_{i,t-1} + b_i s_{i,t-1}. \quad (14)$$

¹²Measures of model fit (such as the ones introduced by [Newton and Raftery, 1994](#); [Spiegelhalter et al., 2002](#)) favors the permanent-transitory decomposition over specifications which only features transitory components.

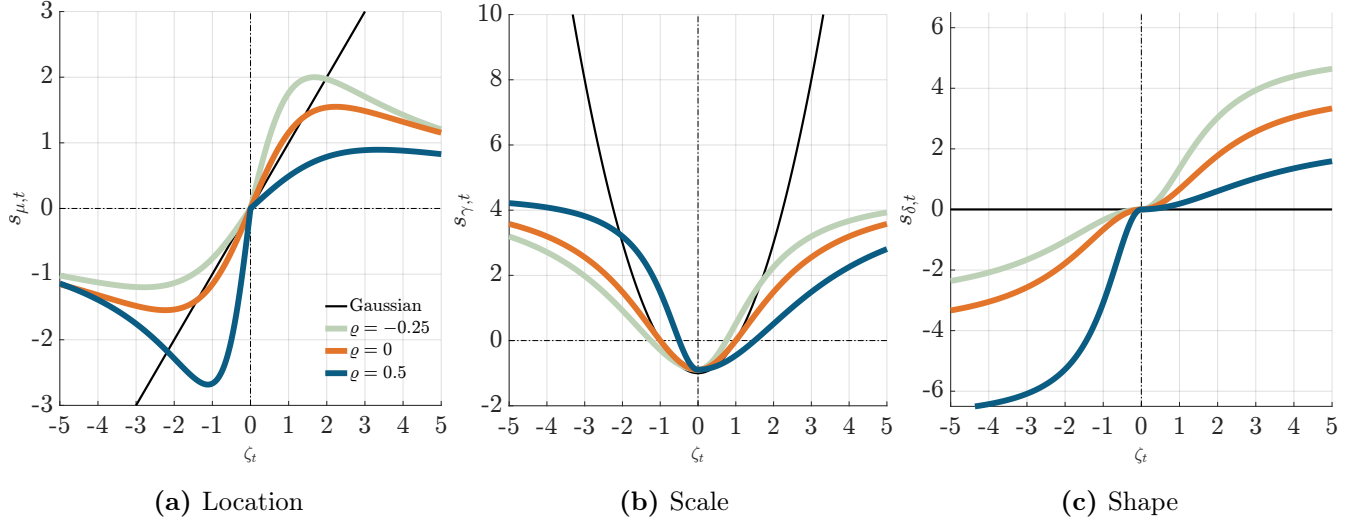


Figure 2: Parameter updating

Note: Note: The panels report the scaled scores for different values of the standardized prediction error $\zeta_t = \frac{\varepsilon_t}{\sigma_t}$. We consider the Gaussian case (black), the symmetric $Skt_5(\mu_t, \sigma_t, 0)$ (orange), and negatively (green) and positively (blue) $Skt_5(\mu_t, \sigma_t, \varrho_t)$.

Updates of the time-varying parameters are proportional to $s_{i,t-1}$, which is the *scaled score* of the conditional distribution (as in [Creal et al., 2013](#); [Harvey, 2013](#)).¹³

Intuitively, the score vector translates the new information contained in the latest data release, summarized by the prediction error, $\varepsilon_t = \pi_t - \mu_t$, into an update for the time-varying parameters characterizing the predictive distribution of inflation; learning rates, a_i and b_i , regulate the strength of the updates.¹⁴ We illustrate the updating mechanism in [Figure 2](#).

Consider a symmetric Gaussian environment (black lines), where $\nu \rightarrow \infty$ and $\varrho_t = 0$ in every period. The location and scale parameters—now corresponding to the mean and standard deviation of the distribution—are updated according to standard Kalman-filter learning. The mean is revised proportionally to the prediction error, with the size of the update inversely related to the volatility of the data (see, e.g., [Cogley, 2002](#)). The volatility is adjusted upward when the squared standardized prediction error exceeds its expected value of one, and downward when it falls below that. Allowing for fat tails makes the updating mechanism robust to large, unanticipated errors

¹³The scaled score vector, $s_t = (s_{\mu,t}, s_{\sigma,t}, s_{\delta,t})'$, is defined as $s_t = \mathcal{S}_t \nabla_t$, where ∇_t is the gradient of the likelihood function with respect to the dynamic parameters; the scaling matrix \mathcal{S}_t is proportional to the inverse of the diagonal of the Information matrix, $\mathcal{I}_t = E[\nabla \nabla']$. Updates driven by the scaled score are (generally) guaranteed to reduce the distance between the conditional and the true (unobserved) predictive distribution, easily allowing for non-Gaussian features. See [Blasques et al. \(2015\)](#)

¹⁴[Appendix D](#) contains detailed derivations for the score and updates of the time-varying parameters of the model.

(orange lines; see. e.g., [Delle Monache and Petrella, 2017](#); [Antolín-Díaz et al., 2024](#)).

When asymmetry is introduced, the updating mechanism weights prediction errors differently depending on their sign and magnitude. For instance, under a left-skewed conditional distribution (green lines), the model places greater emphasis on unexpected positive inflation surprises, while negative errors are viewed as more probable and therefore do not necessarily prompt large revisions in the perceived risk asymmetry. More generally, small (standardized) prediction errors are interpreted as signals about the central scenario and lead to only minor revisions to the shape parameter. In contrast, large deviations from the central forecast are taken as evidence of a shift in the balance of risks, prompting updates to the asymmetry parameter in the direction of the surprise. Consistently with this mechanism, large deviations of inflation from the expected central scenario imply updates of the asymmetry parameter in the direction of the prediction error.

The parameters of the model and the associated conditional distribution of inflation are estimated using Bayesian methods as in [Delle Monache et al. \(2024\)](#); refer to [Appendix D](#) for additional details. An extensive Monte Carlo exercise, reported in [Appendix E](#), demonstrates that the procedure detects skewness only when it is present and remains robust to (changing) correlations between location and scale.

4.2 Time varying skewness of inflation risk

The estimated model provides new insights into the time-varying stochastic properties of the inflation process. While much is already known about the mean and variance of inflation (see, e.g., [Stock and Watson, 2007](#)), our approach sheds light on the dynamics of inflation skewness.¹⁵

Panel (a) of [Figure 3](#) shows the estimated time-varying skewness of inflation. Skewness is moderate negative during the 1960s, followed by rising upside risks beginning in the late 1960s, peaking in the late 1970s, and then gradually declining from the early 1980s. Upside risks persist through the mid-1990s, after which the skewness turns negative. Downside risk dominates from that point until the post-COVID inflationary period, with the exception of the years preceding the Global Financial Crisis (GFC), when risks appear balanced. The model captures a sharp increase

¹⁵Estimates of the time-varying mean and volatility of U.S. core PCE are broadly consistent with those obtained from the [Stock and Watson \(2007, 2016\)](#) framework (see [Appendix F](#) for further analysis).

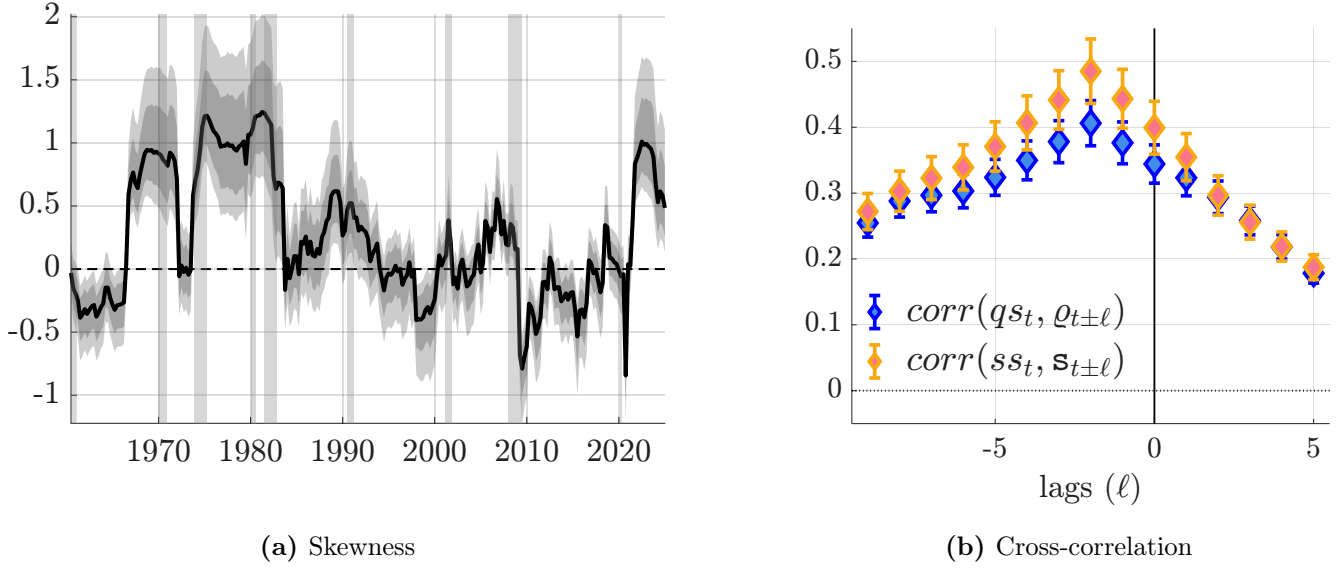


Figure 3: Time-varying asymmetric risks of Core PCE inflation

Note: Panel (a) plots the estimated time-varying skewness of U.S. core PCE inflation, along with 68% and 95% credible intervals. Gray shaded areas indicate NBER recessions. Panel (b) reports the cross-correlations between realized (ex-post) measures of inflation skewness—specifically, the 5-year rolling quantile skewness (qs_t) and the 5-year rolling sample skewness (ss_t)—and our model-based (ex-ante) measure of predictive asymmetry in risk, captured by the asymmetry parameter ϱ_t and the conditional skewness \mathbf{s}_t , respectively.

in negative skewness during the COVID pandemic, followed by a rapid shift toward upside risk. By the end of 2020, significant upside risks emerge, reaching levels by mid-2021 comparable to those observed during the Great Inflation of the 1970s. Notably, the estimated skewness during the recent inflation surge closely mirrors the magnitudes seen in the mid-1970s, while the pre-COVID low-inflation period resembles the stable inflation environment of the 1960s. [Appendix F](#) extends the analysis to alternative measures of inflation, examining inflation rates derived from headline PCE, core and headline CPI, and the GDP deflator. Time-varying asymmetry in risk emerges as a robust feature of inflation, regardless of the price index used. Periods of upside or downside skewed risk tend to align across these indicators. Notably, core PCE inflation appears to exhibit a more attenuated balance of risk compared to other inflation measures.

Assessing how well our model-based measures of asymmetric risks captures changes in inflation risk is inherently challenging, as we only observe a single realization from a time-varying distribution. While ex-post skewness can be gauged using rolling measures derived from the data, these backward-looking estimates face important limitations. Rolling window estimators of skewness strike a trade-off between precision and responsiveness. Longer windows improve statistical re-

liability by smoothing out outliers but reduce the ability to detect rapid changes in risk. They also assume constant skewness within the window, causing delayed adjustments during periods of sharp inflation movements, when timely assessment matters most.

To balance these trade-offs, we use 5-year rolling estimates and consider both sample skewness (ss_t) and quantile skewness (qs_t) as benchmarks. The former can be compared to our model’s conditional skewness measure, \mathbf{s}_t , while the latter is conceptually closer to the asymmetry parameter, ϱ_t , as it captures the imbalance of probability mass around the mode. Unlike rolling statistics, our model applies one-sided discounting of past data to estimate time-varying moments, yielding more responsive and stable signals of inflation risk. [Figure 4](#) shows that our model-based skewness estimates closely track rolling estimates, with maximum cross-correlations between 0.4 and 0.5. Importantly, our estimates consistently lead the rolling measures by about two quarters, providing a timely and reliable signal of changes in the balance of risks—a key advantage for monitoring the evolution of inflation risk.

4.3 Expected value under asymmetry

A defining feature of any skew-distribution, $p(\pi|\mu_t, \sigma_t, \varrho_t, \nu)$, is the fact that asymmetry directly affects the first moment of the distribution. Specifically, in the case of the Skew-t distribution in [Equation \(12\)](#), one can show that $\forall h > 0$

$$E_t \pi_{t+h} = \int_{\mathbb{R}} \pi \times p(\pi|\mu_{t+h}, \sigma_{t+h}, \varrho_{t+h}, \nu) d\pi = \mu_{t+h} + \underbrace{g(\nu)\sigma_{t+h}\varrho_{t+h}}_{\psi_{t+h}} \quad (15)$$

where $g(\nu) = \frac{4\nu\mathcal{C}(\nu)}{\nu-1}$. Therefore, the expected value can be represented as the sum of the mode and a component, ψ_{t+h} , that is a function of the asymmetry parameter. That is, asymmetry creates a wedge between the central scenario (i.e. the mode of the distribution, μ_{t+h}), and the expected value. This wedge has the same sign of the prevalent asymmetry and is quantitatively in more uncertain periods (i.e. when σ_{t+h} is large). When risk is skewed to the upside (i.e. $\varrho_{t+h} > 0$), an increase in risk corresponds to rising inflation expectations. Conversely, when risk is negatively skewed (i.e. $\varrho_{t+h} < 0$), an increase in risk results in a decline in expected inflation.

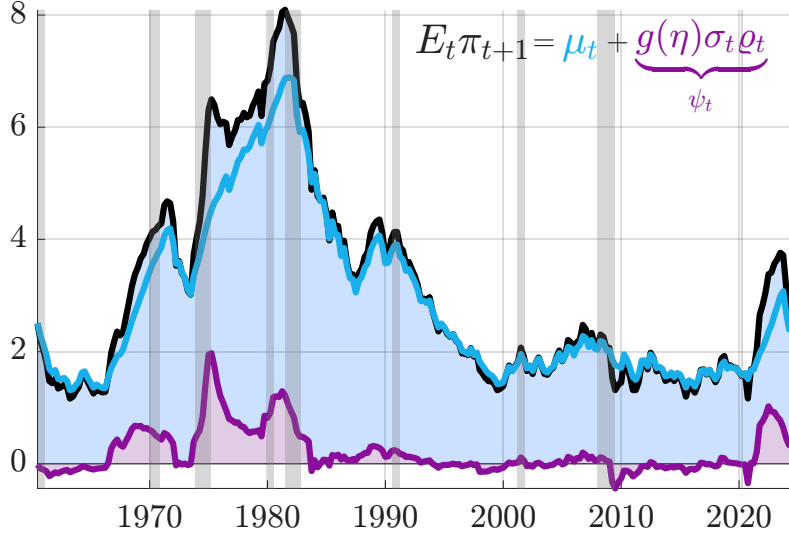


Figure 4: Inflation mean decomposition

Note: The figure reports the decomposition of the model based measure of inflation expectations, reported in Equation (15). The total expectation (in black) is decomposed into a central scenario (μ_t , cyan) and the tilt induced by the balance of risks (ψ_t , purple).

Figure 4 illustrates the decompositions of model based inflation expectations into a central scenario (the most likely expected outcome) and the tilt induced by the balance of risks around it, ψ , which is itself a function of the skewness, based on Equation (15).

Inflation risk significantly influences inflation expectations, especially in periods of high inflationary pressures and price volatility. The high labor costs and rising interest rates of the 1970s and 1980s are consistent with a prevalence of upside risks to inflation. Similarly, recent supply chain disruptions and geopolitical tensions could be associated with positive balance of risks estimated in the last 3 years of the sample.¹⁶ Negative skewness contributed to a downward bias in expected inflation during the decade leading up to the COVID pandemic. Most of the post-Great Financial Crisis period has been characterized by the recurrence of zero lower bound spells, associated to strong deflationary concerns (see, e.g. Adam and Billi, 2007). However, remarkably low inflation volatility during these years mitigated the average effect of asymmetry on expectations, limiting its impact to around 20 basis points, despite the markedly negative skewness. The subdued volatility of inflation observed during this time has significant implications for how monetary policy should address the persistent negative skewness in the post-Great Recession era.

¹⁶De Polis et al. (2023) relate the dynamics of inflation moments to macroeconomic and financial predictors, suggesting that a mix of fiscal and monetary related factors account for the largest share of predictability.

Table 1: Out-of-sample comparison

	MSFE	CRPS	CRPS Decomposition			Event Forecasts		
			Right	Left	Center	$\pi_{t+h} < 1.5$	$1.5 \leq \pi_{t+h} \leq 2.5$	$\pi_{t+h} > 2.5$
h = 1	0.969 (0.011)	0.995 (0.333)	0.998 (0.424)	0.992 (0.186)	0.995 (0.364)	0.956 (0.001)	0.966 (0.004)	0.967 (0.001)
h = 4	0.925 (0.000)	0.958 (0.001)	0.979 (0.052)	0.940 (0.000)	0.954 (0.000)	0.981 (0.107)	0.981 (0.115)	0.987 (0.064)
h = 8	0.884 (0.000)	0.927 (0.000)	0.939 (0.000)	0.921 (0.000)	0.920 (0.000)	0.975 (0.074)	0.970 (0.014)	1.007 (0.702)

Note: The table report the relative performance of [Stock and Watson \(2007\)](#) UCSV model against our Skew- t model. Results are reported in ratios, with our model being at the numerator; values smaller than 1 imply superior predictive accuracy of the Skew- t model. The out-of-sample period runs from 2000Q1 to 2024Q4. Values in **bold** are significant at the 10% level.

4.4 Out-of-sample evaluation

In this section we provide a full scale evaluation of the out-of-sample forecasting performance of our model. We set up a real-time forecasting exercise where for each inflation vintage we produce up to eight-step ahead forecasts for the whole density of core PCE inflation, starting from 2000Q1.¹⁷ We compare our model against the widely used UCSV model of [Stock and Watson \(2007\)](#), in terms of point, density and event forecasts, measured by the mean squared forecast error (MSFE), the Continuously Ranked Probability Score (CRPS) of [Gneiting and Ranjan \(2011\)](#) and the Brier score, respectively.¹⁸ Additional results are available in [Appendix C](#).

The comparison strongly favors our model, across all metrics and forecast horizons, as presented in [Table 1](#). The results, expressed as the ratio of the score achieved by our model to that of the UCSV benchmark, show significant gains in point forecasts range from 3% at short horizons to 10% over the medium term, where p-values for the [Diebold and Mariano \(1995\)](#) test are provided in parentheses. Improvements of up to 7% are observed in CRPS scores. Substantial gains are also reported for the predictions of events where π_{t+h} is lower than 1.5%, greater than 2.5%, or falls within these thresholds. These results underline the importance of accounting for inflation skewness as a means to enhance forecasting accuracy.

¹⁷We start the exercise in 2000Q1 due to the availability of real-time data vintages.

¹⁸The Continuously Ranked Probability Score (CRPS) scoring rule measure the squared difference between the predictive distribution function and the “perfect forecast”. This score can be modified to highlight different regions of the predictive density (see, e.g. [Gneiting and Ranjan, 2011](#)).

The UCSV model lacks a mechanism for capturing skewness and overlooks the presence of fat tails in the data. Replicating the exercise using a specification that excludes asymmetry (similarly to [Delle Monache and Petrella, 2017](#)) confirms the importance of incorporating skewness to improve model fit and inflation forecasting accuracy (see also [Mouabbi et al., 2025](#)).¹⁹

[Adams et al. \(2021\)](#) show that both upside and downside risks to the median SPF forecast fluctuate over time, and that lower quantiles of the predictive distributions are generally more stable than the upper quantiles. We find our model to perform on par with the SPF.²⁰ Notably, for $P\left(\pi_{t+1}^{Q4} > 2.5\%\right)$ our model shows meaningful advantages, stemming from consistently lower event probability assessments compared to the SPF during the decade following the Great Recession, and a timely adjustment in early 2022, anticipating the inflation spike of the post-COVID period.

5 Quantitative structural analysis

In this section, we assess the quantitative relevance of shifts in the balance of inflation risk using the empirical DSGE model of [Smets and Wouters \(2007\)](#) augmented with asymmetric shocks. We explore the macroeconomic implications of implementing a central bank communication strategy aimed at anchoring expectations by offsetting the effects of asymmetric risks. Focusing on the post-pandemic period, we compare the effects of the RAIT with those of the FAIT, currently employed by the Federal Reserve.

5.1 Macroeconomic effects of shifts in the balance of risk

To assess the macroeconomic impact of shifts in the balance of inflation risk, we cast the model by [Smets and Wouters \(2007\)](#) into its beliefs representation, which was defined in [Section 2.2](#). In this representation, the model is endowed with dummy surprise and news shocks to reflecting the revisions to expectations associated with changing risk perceptions.

We assume that time variation in inflation risk stems from changes in expectations about future

¹⁹These results are reported in [Table C4](#) in [Appendix C](#).

²⁰We compare forecasts for the Q4-over-Q4 core PCE, which is the measure predicted by the SPF. The evaluation sample starts in 2007Q1 to match SPF data.

cost-push shocks.²¹ These structural shocks are assumed to follow a Skew- t distribution with time-varying moments. As in the theoretical model of [Section 2](#), agents receive news about the skewness of these shocks up to $J = 20$ quarters ahead.

In the beliefs representation, the inflation Phillips Curve of this model with asymmetric cost-push shocks reads as follows:

$$\hat{\pi}_t = \pi_1 \hat{\pi}_{t-1} + \pi_2 E_t \hat{\pi}_{t+1} - \pi_3 \mu_t^p + \varepsilon_t^p + \sum_{j=0}^J \varphi_{t-j}^j, \quad (16)$$

where μ_t^p represents firms' mark-ups, ε_t^p is the actual cost-push shock, and φ_{t-j}^j are dummy cost-push shock revealed at time $t-j$ and expected to materialize j periods ahead. These dummy shocks tilt the expected path of future shocks to capture the effects of changing skewness on expectations.

The model's solution follows a standard linear form:

$$\mathbf{s}_t = \Gamma \mathbf{s}_{t-1} + \Omega \mathbf{e}_t, \quad (17)$$

where \mathbf{s}_t includes all state variables and \mathbf{e}_t captures structural shocks and dummy shocks. The solution matrices Γ and Ω depend on the model's structural parameters. The model cast in this form can be solved with fast, off-the-shelf techniques.

We use this framework to simulate the macroeconomic effects of a shift in the balance of risks. The parameter values are set to their estimated values as reported by [Smets and Wouters \(2007\)](#) based on U.S. data. We consider two hypothetical scenarios, both involving an increase in upside risk. The first features a sharp but short-lived rise in risk; the second entails a more persistent revision, where risk builds gradually before subsiding. The top-left panel of [Figure 5](#) displays the sequence of dummy shocks used in each case, while the remaining panels show the responses of inflation, the policy rate, and hours worked. The size of the dummy shocks reflects the mean shift in expected cost-push shocks due to increased upside risks. This corresponds to a jump in expected cost-push shocks of roughly one fourth of the estimated standard deviation of these shocks—an

²¹This setup can be generalized to accommodate alternative identification assumptions by incorporating a variety of dummy shocks that contribute to alternative revisions in risks.

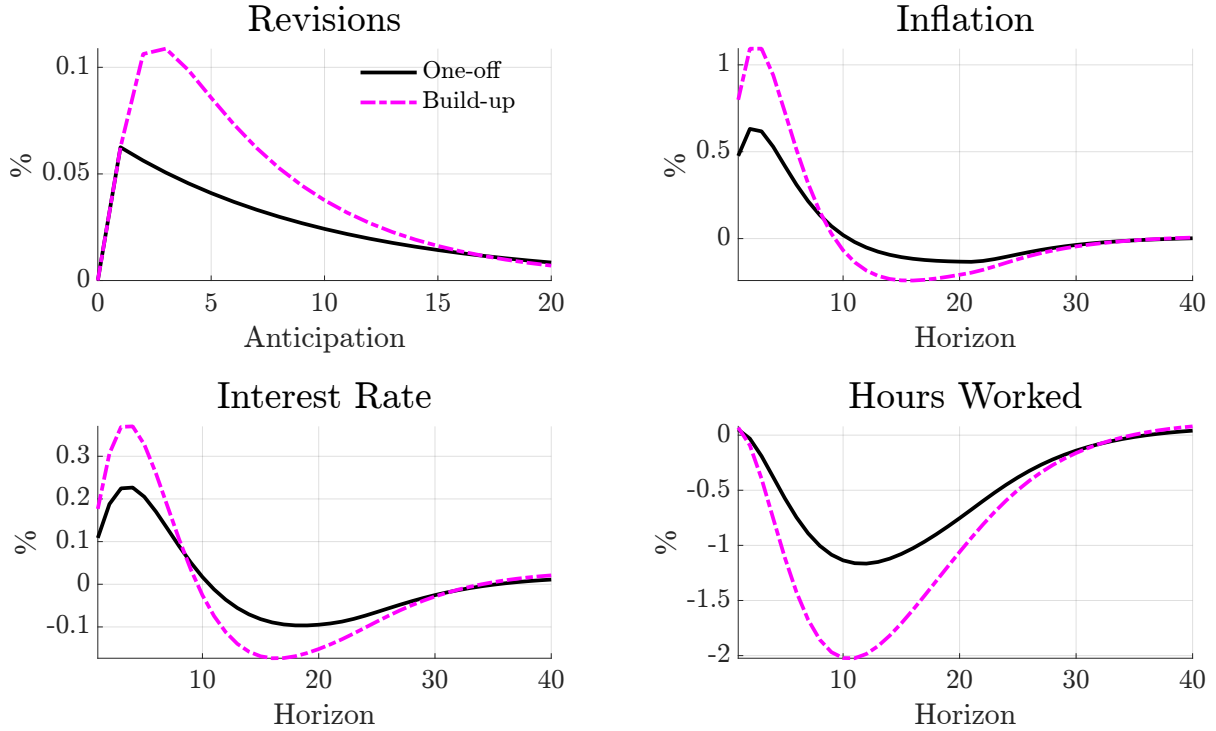


Figure 5: Impulse response function to an increase in expected upside risk to inflation

Note: The top left panel reports the path of the revisions to the expected upside risks to inflation, anticipated over up to 20 periods. The remaining panels report the response of inflation, the interest rate and hours worked to such revision shocks. We assume two possible paths for the revisions: a persistent one-off shock, reported in black, and a slower and persistent build-up, in magenta.

amount broadly consistent with the size of standard forecast revisions in the post-2000 sample, as discussed in [Section 4.2](#).²²

In both scenarios, upside-skewed cost-push shocks raise agents’ expectations of future inflation. Firms able to reoptimize their prices incorporate these expectations into current pricing decisions, resulting in higher inflation today. This, in turn, triggers a monetary policy response—even though the central bank does not directly react to the shift in the balance of inflation risks, but rather to the resulting inflationary pressure arising through the expectations channel. Higher prices and tighter policy slow economic activity, as reflected in the hump-shaped decline in total hours worked. As demand weakens, disinflation sets in: inflation gradually declines, slightly undershoots the target, and eventually returns to it.

The two scenarios highlight that the macroeconomic consequences of shifts in risk are both

²²The revision paths considered represent hypothetical scenarios. The empirical model in [Section 4.2](#) typically generates monotonic revisions, similar to the “one-off” scenario. However, one can also envision situations where a delayed policy announcement leads to a gradual “build-up” of skewed risk. In this case, the “build-up” scenario corresponds to an environment where perceived risk peaks three quarters after the announcement.

substantial and persistent, and they illustrate the trade-off faced by monetary policy: higher inflation versus weaker demand. In the build-up scenario, the more persistent revision in risks calls for a tighter policy response, which initially deepens the contraction in real activity as the central bank attempts to contain inflationary pressures.

5.2 Risk-Adjusted Inflation Targeting

We now introduce a central bank communication strategy aimed at anchoring expectations by offsetting the effects of asymmetric risks: the RAIT. This monetary policy strategy aims at tilting the path for expected inflation in the direction opposite of the perceived inflation risk. When the balance of risks signals upward (downward) inflation pressure, the central bank temporarily aims to undershoot (overshoot) its target. This approach reflects the core insight from our theoretical model in [Section 3](#): the central bank should lean against upside inflation risks and adopt a more accommodative stance when downside risks dominate.

To implement the RAIT, we add a time-varying inflation target to the monetary policy rule:

$$\hat{r}_t = \rho \hat{r}_{t-1} + (1 - \rho) \left[r_x \hat{x}_t + r_{\Delta x} \Delta \hat{x}_t + r_{\pi} \left(\hat{\pi}_t - \underbrace{\sum_{j=1}^J \hat{\pi}_{t-j}^*}_{\hat{\pi}_t^{\text{RAIT}}} \right) \right] + \varepsilon_t^r, \quad (18)$$

where \hat{r}_t and \hat{x}_t are log deviations from steady state of the nominal interest rate and the output gap, respectively. The coefficients are specified as in [Smets and Wouters \(2007\)](#). The term $\hat{\pi}_{t-j}^*$ captures past communication regarding the central bank's intention to over- or undershoot the inflation target in response to perceived risks. $\hat{\pi}_t^{\text{RAIT}}$ reflects the net deviation from the target announced at time t . A negative (positive) value of $\hat{\pi}_{t+h}^{\text{RAIT}}$ signals intentions to undershoot (overshoot) the target h periods ahead. The long-run inflation target is calibrated to 2% annually.

The central bank can implement the RAIT without explicitly communicating a temporary over- or undershooting of the inflation target. The guidance shocks $\{\hat{\pi}_{t+j|t}^*\}_{j=1}^J$, rescaled by $-(1 - \rho)r_{\pi}$, can be seen as stochastic shifts in the intercept of the policy rule, shaping the expected path of interest rates. In this case, the implementation of the RAIT resembles forward guidance—that

is, communication about the likely path of policy rates. Under the RAIT, these shifts represent the central bank’s assessment of the balance of inflation risks and indicate the adjustment in the reaction function required to offset risk asymmetries.

Under the RAIT, the central bank updates the communication about path of future interest rates in response to changes in the balance of risks. Forward guidance is used to neutralize the impact of changing asymmetric risks on inflation expectations. Specifically, the central bank commits to temporary deviations from the statutory target by selecting a sequence $\{\pi_{t+j|t}^*\}_{j=1}^J$ such that the following condition is satisfied:

$$E[\pi_{t+h} | \{\varphi_t^j\}_{j=1}^J] + E[\pi_{t+h} | \{\pi_{t+j|t}^*\}_{j=1}^J] = 0, \quad (19)$$

for $h = 1, \dots, J$, where $E[\pi_{t+h} | \{x_t^j\}_{j=1}^J]$ denotes the effect of a revision in x , j periods into the future, on expected inflation h periods ahead. Hence, with the RAIT-based guidance, average inflation converges to the target over the forecast horizon, as the effects of skewness on inflation expectations are fully neutralized by the strategy.

Forward guidance puzzle? The RAIT can be thought of as being implemented through forward guidance shocks—that is, anticipated monetary policy shocks, $\hat{\pi}_{t|t-j}^*$. While the literature has identified the forward guidance puzzle—namely, the implausibly strong effects of forward guidance in standard models—this issue does not arise here. As shown by [Maliar and Taylor \(2019\)](#); [Del Negro, Giannoni, and Patterson \(2023\)](#); [Bianchi, Melosi, and Nicolò \(2024\)](#), the puzzle typically emerges when forward guidance shocks are used to match a pre-set interest rate path, thereby shutting down the endogenous policy response. In contrast, the RAIT relies on forward guidance shocks to restore inflation expectations—distorted by asymmetric risks—back to target, while preserving the endogenous feedback of monetary policy and thereby avoiding the puzzle.

5.3 Policy Counterfactual

In this section, we present policy counterfactuals to evaluate the RAIT during the post-pandemic period. Any counterfactual policy analysis requires as input a revision in the balance

of future risks. These revisions can be judgment-e.g. based—reflecting the policymaker’s subjective view—or derived from model-based estimates. We adopt the latter approach and detail the mapping from inflation risk to the beliefs representation in the next subsection.

5.3.1 Calibrating Inflation Risk and the RAIT

For simplicity, we assumed that the only source of inflation risk asymmetry stems from cost-push shocks. We calibrate the dummy anticipated cost-push shocks to match the effects of the revisions in the balance of inflation risks on inflation expectations, $\psi_{t+h|t} - \psi_{t+h|t-1}$, where $\psi_{t+h|t} = E_t \pi_{t+h} - \mu_{t+h|t}$, estimated using the Skew- t model of [Section 4](#). See [Equation \(15\)](#). This requires solving the following system of $J + 1$ linear equations:

$$\begin{bmatrix} -\sum_{j=1}^J \varphi_{t-j}^j \\ \psi_{t+1|t} - \psi_{t+1|t-1} \\ \vdots \\ \psi_{t+J|t} - \psi_{t+J|t-1} \end{bmatrix} = \begin{bmatrix} 1 & \mathbf{0}_{1 \times J} \\ \Omega^S & \Omega^N \end{bmatrix} \begin{bmatrix} \varphi_t^0 \\ \varphi_t^1 \\ \vdots \\ \varphi_t^J \end{bmatrix}, \quad (20)$$

where Ω^S and Ω^N capture the effects of surprise and anticipated dummy cost-push shocks on inflation expectations in [Equation \(17\)](#). These matrices are derived from the solution of the Smets and Wouters model with dummy cost-push shocks—[Equation \(17\)](#). This solution is straightforward to obtain using widely available techniques. Inverting the matrix on the right-hand side yields the dummy shocks, $\{\varphi_t^j\}_{j=1}^J$ that ensure the structural model replicates the estimated effects of skewness on inflation expectations.

The first equation ensures dummy anticipated shocks do not materialize as actual cost-push shocks.²³ As explained in [Proposition 2](#), these dummy shocks represent belief distortions and can be interpreted as pure beliefs or sentiments. The remaining equations map the revisions to inflation expectations—arising from the inflation asymmetry estimated in real time by the Skew- t model—onto belief shocks. This final set of equations pins down the anticipated dummy shocks required to shift expectations in line with the estimated changes in perceived risk at each horizon.

²³The surprise shock needed to neutralize past anticipated shocks affects inflation expectations, which one has to take into account. These effects are captured by the vector $\Omega^S \varphi_t^0$.

Similarly, the sequence of forward guidance shocks $\{\hat{\pi}_{t+j|t}^*\}_{j=1}^J$ in [Equation \(19\)](#):

$$\begin{bmatrix} \psi_{t+1|t} - \psi_{t+1|t-1} \\ \psi_{t+2|t} - \psi_{t+2|t-1} \\ \vdots \\ \psi_{t+J|t} - \psi_{t+J|t-1} \end{bmatrix} = -\Omega^{FG} \begin{bmatrix} \hat{\pi}_{t+1|t}^* \\ \hat{\pi}_{t+2|t}^* \\ \vdots \\ \hat{\pi}_{t+J|t}^* \end{bmatrix}, \quad (21)$$

where the $J \times J$ matrix Ω^{FG} captures the effect of forward guidance shocks on inflation expectations. This matrix, Ω_{FG} , is obtained by solving the beliefs representation of the [Smets and Wouters \(2007\)](#) model, augmented with the RAIT-based monetary policy rule [Equation \(18\)](#).

The left-hand side of the system in [Equation \(21\)](#) shows the impact of estimated risk revisions on inflation expectations, while the right-hand side represents the forward guidance shocks needed to neutralize that impact. These shocks can be easily obtained by inverting the matrix Ω_{FG} . Solving this linear system ensures that forward guidance neutralizes the effects of the revised balance of inflation risks on expectations, thereby anchoring them as intended under the RAIT.

5.3.2 The RAIT in the post-pandemic inflation

We use the [Smets and Wouters \(2007\)](#) model augmented with asymmetric cost-push shocks to assess how the RAIT would have changed the post-pandemic macroeconomic dynamics in the US. As before, we set all parameters in line with the posterior estimates of [Smets and Wouters \(2007\)](#). Under this calibration, the Phillips curve slope is approximately 0.03 over the 1966–2004 period, which contrasts with more recent evidence suggesting a significantly steeper slope during the latest inflation surge. In light of this, we set the relevant parameters to match a slope of 0.3.

The model explains U.S. data using all shocks, including the dummy shocks calibrated to match the first-order effects of real-time changes in the skewness of cost-push shocks, as estimated by the Skew- t model. To quantify the effects of having followed the RAIT in the post-pandemic period, one simply needs to simulate the [Smets and Wouters \(2007\)](#) model using only the forward guidance shocks derived from the procedure described in [Section 5.3](#), based on real-time revisions in the balance of inflation risks. This procedure is valid due to the linearity of the model and the

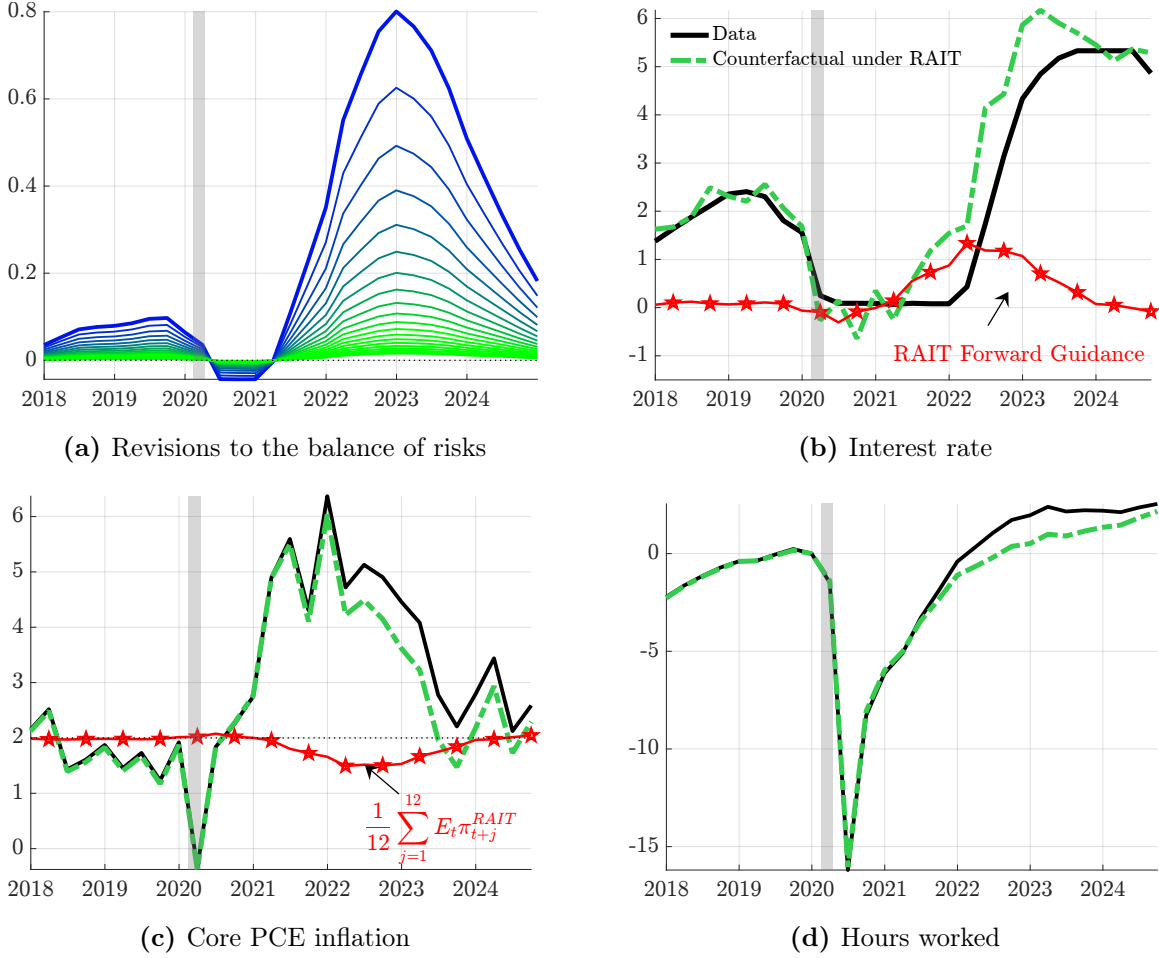


Figure 6: Macro dynamics under the RAIT

Note: The plots report the estimated revisions to the balance of inflation risks and the counterfactual dynamics of the policy rate, inflation and hours worked consistent with the RAIT framework, against the actual data (black). Inflation is defined as annualized quarter-on-quarter core PCE. Hours worked are the logarithm of hours worked in the nonfarm business sector, normalized to 0 in 2019Q4. Panel (b) also includes the forward guidance component of future monetary policy under RAIT, calculated as $-(1 - \rho)r_\pi \frac{1}{12} \sum_{j=1}^{12} \hat{\pi}_{t|t+j}^*$. Panel (c) also displays the expected average RAIT target over the next three years, $\frac{1}{12} \sum_{j=1}^{12} E_t \pi_{t+j}^{RAIT}$. Gray shaded areas represent NBER recessions.

orthogonality of the shocks involved.

Figure 6 shows the RAIT-implied federal funds rate, core PCE inflation, and hours worked, alongside actual data. Panel (a) displays the estimated revisions to inflation risk, $\{\psi_{t+h|t} - \psi_{t+h|t-1}\}_{h=1}^{20}$, which forward guidance under the RAIT dynamics counteract. These estimates indicate that signs of upside inflation risk began emerging since early 2021, with sustained revisions through the end of 2023.

Following a sharp increase in inflation risks, the RAIT would have called for a rapid tightening as early as 2021. Compared to the observed policy path, the interest rate implied by the RAIT

is consistently higher, reflecting the model’s recommendation to adopt a tighter stance earlier—whereas the Fed’s actual hiking cycle began roughly three quarters later. Similarly, as the positive asymmetry of inflation began to decline in 2023, the RAIT would have favored an earlier easing.

Remarkably, at the peak of the response, the RAIT prescribes a policy rate broadly in line with the rate eventually set by the FOMC. Thus, the main difference lies in timing: the RAIT would have initiated tightening sooner and reached its peak two quarters earlier.

Overall, the RAIT prescribes a more proactive policy—tightening preemptively when upside risks emerge and easing more swiftly as risks subside or give way to downside risks. As a result of the more responsive stance, inflation expectations remain anchored, and inflation would have returned to target about a year earlier. Labor market conditions initially weaken through 2022 and much of 2023, before regaining momentum in response to the anticipated easing later in 2023.

The RAIT policy includes a forward guidance component. In response to positive *revisions* in perceived upside inflation risk, the central bank not only raises interest rates but also signals future increases to mitigate the impact of skewed risks on inflation expectations. Based on our real-time estimates, the shift in risk begins in the second quarter of 2021 and leads the RAIT to recommend increasingly hawkish communications throughout the remainder of 2021 and into early 2023 (see Panel b). By the end of 2021, the central bank would have raised rates by 150 basis points and signaled at least three additional hikes for the following year. As inflation risks subside, forward guidance under the RAIT moderates in 2023, becoming neutral by 2024, consistent with a more balanced risk outlook.

5.3.3 RAIT vs FAIT

Forward guidance under the RAIT framework reflects the central bank’s commitment to respond to inflation deviations from a *time-varying target*, π_t^{RAIT} (see [Equation \(18\)](#)). Revisions in perceived inflation risk lead to policy communications aligned with an *implicit* adjusted inflation target. Positive (negative) deviations from the 2% statutory target are required to offset perceived increases in downside (upside) inflation risk.

The Fed’s current policy framework, the FAIT, allows for temporary inflation overshoots to

offset past negative misses of inflation (Clarida, 2022).²⁴ Like the RAIT, the FAIT seeks to steer inflation expectations by influencing the distribution of expected inflation. However, the two frameworks differ in how they condition overshooting or undershooting. Under the FAIT, the central bank adjusts its stance based on past inflation misses—implicitly treating them as proxies for current and future risks. In contrast, the RAIT bases communication on forward-looking risk assessments: the central bank commits to overshoot (undershoot) the target when risks are skewed to the downside (upside). As a result, the FAIT is inherently backward-looking and potentially one-sided, whereas the RAIT is forward-looking and symmetric.

Appendix G compares the inflation target implied by the FAIT and the RAIT over the post-2000 period. This comparison highlights the key differences between the two strategies. Focusing on the post-pandemic inflation surge, the FAIT’s backward-looking design causes its implicit target to lag behind the RAIT’s target, limiting its responsiveness to rapidly shifting inflation risks. As a result, the FAIT signals policy tightening too late and fails to recognize the swift normalization of risks by the end of the sample. In contrast, the RAIT’s forward-looking approach supports an earlier adjustment, justifying monetary easing as early as 2023 based on real-time risk assessments from our model in Section 4.

FAIT may provide extreme policy response in the aftermath of persistent deviations of inflation from target, requiring substantial adjustments to the inflation target to offset past misses. For example, while RAIT recommends a tighter policy stance and communications consistent with only a temporary undershoot of the 2% statutory target—by up to 30 basis points—as inflation rises in 2022 (see Figure 6, Panel (c)), alternative calibrations of FAIT would call for a significantly larger undershoot of at least 100 basis points. Moreover, under FAIT, this deviation would persist even after inflation has largely retrenched by the end of 2024. In contrast, under RAIT, the policy target re-aligns with the 2% statutory goal by the end of the sample.

²⁴The version adopted in August 2020 was asymmetric, with no explicit provision for undershooting the inflation target.

6 Concluding remarks

This paper investigates the role of time-varying inflation skewness in macroeconomic dynamics. Moreover, we show that when inflation risks are asymmetric, it is optimal for the central bank to lean against the balance of inflation risks.

We introduce a tractable framework that captures how asymmetric cost-push shocks propagate through agents' beliefs. The mechanism operates by augmenting a linear model with a sequence of anticipated dummy shocks that inform agents about the evolving asymmetry in cost-push shocks. The model remains linear, preserving both tractability and interpretability.

Using a time-series model to estimate the predictive distribution of U.S. core PCE inflation, we document substantial fluctuations in inflation skewness over time. These shifts affect the balance of risks and improve forecast accuracy during periods of heightened volatility.

Finally, we employ a quantitative model to assess how changes in inflation skewness shape expectations and to evaluate a novel monetary policy strategy—the RAIT—designed to neutralize these effects and anchor expectations more effectively.

References

- ADAM, K. AND R. M. BILLI (2007): “Discretionary monetary policy and the zero lower bound on nominal interest rates,” *Journal of monetary Economics*, 54, 728–752.
- ADAMS, P. A., T. ADRIAN, N. BOYARCHENKO, AND D. GIANNONE (2021): “Forecasting macroeconomic risks,” *International Journal of Forecasting*, 37, 1173–1191.
- ANDRADE, P., E. GHYSELS, AND J. IDIER (2014): “Inflation risk measures and their informational content,” *Available at SSRN 2439607*.
- ANGELETOS, G.-M. AND J. LA’O (2010): “Noisy business cycles,” *NBER Macroeconomics Annual*, 24, 319–378.
- ANTOLÍN-DÍAZ, J., T. DRECHSEL, AND I. PETRELLA (2024): “Advances in nowcasting economic activity: The role of heterogeneous dynamics and fat tails,” *Journal of Econometrics*, 238.
- ARELLANO-VALLE, R. B., H. W. GÓMEZ, AND F. A. QUINTANA (2005): “Statistical inference for a general class of asymmetric distributions,” *Journal of Statistical Planning and Inference*, 128, 427–443.
- ASCARI, G. AND A. M. SBORDONE (2014): “The macroeconomics of trend inflation,” *Journal of Economic Literature*, 52, 679–739.
- BERNANKE, B. S. (2024): “Forecasting for Monetary Policy Making and Communication at the Bank of England: A Review,” Tech. rep., Bank of England, Independent Evaluation Office.
- BIANCHI, F., L. MELOSI, AND G. NICOLÒ (2024): “Is There a Forward Guidance Puzzle?” BSE mimeo, Barcelona.
- BIANCHI, F., L. MELOSI, AND M. ROTTNER (2021): “Hitting the elusive inflation target,” *Journal of Monetary Economics*, 124, 107–122.
- BLASQUES, F., S. J. KOOPMAN, AND A. LUCAS (2015): “Information-theoretic optimality of observation-driven time series models for continuous responses,” *Biometrika*, 102, 325–343.

- CHAHROUR, R. AND K. JURADO (2018): “News or Noise? The Missing Link,” *American Economic Review*, 108, 1702–36.
- CLARIDA, R., J. GALI, AND M. GERTLER (1999): “The Science of Monetary Policy: A New Keynesian Perspective,” *Journal of Economic Literature*, 37, 1661–1707.
- CLARIDA, R. H. (2022): “The Federal Reserve’s New Framework: Context and Consequences,” Finance and Economics Discussion Series 2022-001, Board of Governors of the Federal Reserve System.
- COGLEY, T. (2002): “A Simple Adaptive Measure of Core Inflation,” *Journal of Money, Credit and Banking*, 34, 94–113.
- COGLEY, T. AND T. J. SARGENT (2005): “Drifts and volatilities: monetary policies and outcomes in the post WWII US,” *Review of Economic Dynamics*, 8, 262–302.
- CREAL, D., S. J. KOOPMAN, AND A. LUCAS (2013): “Generalized autoregressive score models with applications,” *Journal of Applied Econometrics*, 28, 777–795.
- DE POLIS, A., L. MELOSI, AND I. PETRELLA (2023): “The ever-changing challenges to price stability,” in *12th European Central Bank Conference on Forecasting Techniques*.
- DEL NEGRO, M., M. P. GIANNONI, AND C. PATTERSON (2023): “The Forward Guidance Puzzle,” *Journal of Political Economy Macroeconomics*, 1, 43–79.
- DELLE MONACHE, D., A. DE POLIS, AND I. PETRELLA (2024): “Modeling and forecasting macroeconomic downside risk,” *Journal of Business & Economic Statistics*, 42, 1010–1025.
- DELLE MONACHE, D. AND I. PETRELLA (2017): “Adaptive models and heavy tails with an application to inflation forecasting,” *International Journal of Forecasting*, 33, 482–501.
- DIEBOLD, F. X. AND R. S. MARIANO (1995): “Comparing predictive accuracy,” *Journal of Business & Economic Statistics*, 20, 134–144.

- DOLADO, J., P. R. MARÍA-DOLORES, AND F. J. RUGE-MURCIA (2004): “Nonlinear Monetary Policy Rules: Some New Evidence for the U.S,” *Studies in Nonlinear Dynamics & Econometrics*, 8, 1–34.
- EVANS, C., J. FISHER, F. GOURIO, AND S. KRANE (2020): “Risk Management for Monetary Policy Near the Zero Lower Bound,” Conference draft, Brooking Paper on Economic Activity.
- FAUST, J. AND J. H. WRIGHT (2013): “Forecasting inflation,” in *Handbook of Economic Forecasting*, Elsevier, vol. 2, 2–56.
- FECHNER, G. T. (1897): *Kollektivmasslehre*, Engelmann.
- FERNÁNDEZ, C. AND M. F. STEEL (1998): “On Bayesian modeling of fat tails and skewness,” *Journal of the American Statistical Association*, 93, 359–371.
- GALÍ, J. (2008): *Monetary Policy, Inflation, and the Business Cycle: An Introduction to the New Keynesian Framework*, Princeton University Press.
- GIANNONI, M. AND M. WOODFORD (2004): “Optimal inflation-targeting rules,” in *The inflation-targeting debate*, University of Chicago Press, 93–172.
- GNEITING, T. AND R. RANJAN (2011): “Comparing density forecasts using threshold-and quantile-weighted scoring rules,” *Journal of Business & Economic Statistics*, 29, 411–422.
- HARVEY, A. C. (2013): *Dynamic models for volatility and heavy tails: with applications to financial and economic time series*, vol. 52, Cambridge University Press.
- HILSCHER, J., A. RAVIV, AND R. REIS (2022): “How likely is an inflation disaster?” CEPR Discussion Papers 17224, C.E.P.R. Discussion Papers.
- KILIAN, L. AND S. MANGANELLI (2007): “Quantifying the risk of deflation,” *Journal of Money, Credit and Banking*, 39, 561–590.
- (2008): “The central banker as a risk manager: Estimating the Federal Reserve’s preferences under Greenspan,” *Journal of Money, Credit and Banking*, 40, 1103–1129.

- KOROBILIS, D., B. LANDAU, A. MUSSO, AND A. PHELLA (2021): “The time-varying evolution of inflation risks,” Working Paper Series 2600, European Central Bank.
- LE BIHAN, H., D. LEIVA-LEÓN, AND M. PACCE (2024): “Underlying inflation and asymmetric risks,” *Review of Economics and Statistics*, 1–45.
- LÓPEZ-SALIDO, D. AND F. LORIA (2024): “Inflation at risk,” *Journal of Monetary Economics*, 145.
- MALIAR, L. AND J. B. TAYLOR (2019): “Forward Guidance: Is It Useful Away from the Lower Bound?” NBER Working Papers 26053, National Bureau of Economic Research, Inc.
- MANZAN, S. AND D. ZEROM (2013): “Are macroeconomic variables useful for forecasting the distribution of US inflation?” *International Journal of Forecasting*, 29, 469–478.
- (2015): “Asymmetric quantile persistence and predictability: the case of US inflation,” *Oxford Bulletin of Economics and Statistics*, 77, 297–318.
- MOUABBI, S., J.-P. RENNE, AND A. TSCHOPP (2025): “Inflation and Growth Risk: Balancing the Scales with Surveys,” *Available at SSRN 5274480*.
- NEWTON, M. A. AND A. E. RAFTERY (1994): “Approximate Bayesian inference with the weighted likelihood bootstrap,” *Journal of the Royal Statistical Society Series B: Statistical Methodology*, 56, 3–26.
- SMETS, F. AND R. WOUTERS (2007): “Shocks and frictions in US business cycles: A Bayesian DSGE approach,” *American economic review*, 97, 586–606.
- SPIEGELHALTER, D. J., N. G. BEST, B. P. CARLIN, AND A. VAN DER LINDE (2002): “Bayesian measures of model complexity and fit,” *Journal of the Royal Statistical Society: Series B (Statistical Methodology)*, 64, 583–639.
- STOCK, J. H. AND M. W. WATSON (2007): “Why has US inflation become harder to forecast?” *Journal of Money, Credit and Banking*, 39, 3–33.

- (2016): “Core inflation and trend inflation,” *Review of Economics and Statistics*, 98, 770–784.
- SURICO, P. (2007): “The Fed’s monetary policy rule and U.S. inflation: The case of asymmetric preferences,” *Journal of Economic Dynamics and Control*, 31, 305–324.
- SVENSSON, L. E. (1997): “Inflation forecast targeting: Implementing and monitoring inflation targets,” *European Economic Review*, 41, 1111–1146.
- SVENSSON, L. E. O. (2003): “What is wrong with Taylor rules? Using judgment in monetary policy through targeting rules,” *Journal of Economic Literature*, 41, 426–477.
- WOODFORD, M. (2003): *Interest and prices*, Princeton University Press Princeton.

A Proofs

A.1 Log-linearized model with asymmetric risk

Let \mathbf{Z}_t collect endogenous and (persistent) exogenous variables, and $\boldsymbol{\varepsilon}_t$ be a vector of i.i.d. exogenous shocks to the system. A stable Rational Expectations equilibrium is defined as a system of expectational difference equations of the form

$$E_t [f(\mathbf{Z}_{t+1}, \mathbf{Z}_t, \mathbf{Z}_{t-1}, \boldsymbol{\varepsilon}_t)] = 0, \quad (\text{A1})$$

where f depends on agents' preferences, available technology, and constraints, and \mathbb{E}_t denotes the expectation operator conditional on the information set available at time t .

Let us now assume $\boldsymbol{\varepsilon}_t = \exp(\boldsymbol{\varepsilon}_t)$ and $\boldsymbol{\varepsilon}_t = [\boldsymbol{\varepsilon}_t^s, \varepsilon_t^a]'$, where $\boldsymbol{\varepsilon}_t^s$ is a set of symmetric shocks—e.g., Normally distributed—while ε_t^a represents a potentially asymmetric shock with distribution. While we focus on the case with a single source of asymmetric risk, extending the analysis to multiple independent asymmetric shocks is straightforward and does not alter the underlying intuition.

Define $\boldsymbol{\varepsilon}^*$ and \mathbf{Z}^* as the steady-state of the model. The first-order Taylor expansion of [Equation \(A1\)](#) around the (non-stochastic) steady state reads

$$\begin{aligned} f(\mathbf{Z}_{t+1}, \mathbf{Z}_t, \mathbf{Z}_{t-1}, \boldsymbol{\varepsilon}_t) &\approx f_{\mathbf{Z}_{t+1}}(\boldsymbol{\varepsilon}^*, \mathbf{Z}^*)(\mathbf{Z}_{t+1} - \mathbf{Z}^*) + f_{\mathbf{Z}_t}(\boldsymbol{\varepsilon}^*, \mathbf{Z}^*)(\mathbf{Z}_t - \mathbf{Z}^*) \\ &\quad + f_{\mathbf{Z}_{t-1}}(\boldsymbol{\varepsilon}^*, \mathbf{Z}^*)(\mathbf{Z}_{t-1} - \mathbf{Z}^*) + f_{\boldsymbol{\varepsilon}_t}(\boldsymbol{\varepsilon}^*, \mathbf{Z}^*)(\boldsymbol{\varepsilon}_t - \boldsymbol{\varepsilon}^*). \end{aligned}$$

where for any generic variable \mathbf{X} , $f_{\mathbf{X}}(\mathbf{X}) = \frac{\partial f(\cdot)}{\partial \mathbf{X}}$ evaluated at \mathbf{X} . Defining log-deviations from steady-states with lower case letters and normalizing $\boldsymbol{\varepsilon}^* = \mathbf{1}$ regardless of the specific shape of the asymmetry of risk, we obtain a linear rational model of the form in [Equation \(1\)](#).

A.2 Proof of [Proposition 1](#)

Proof. Starting from a linear solution of the form in [Equation \(1\)](#):

$$\mathbf{A}_0 \mathbf{z}_t = \mathbf{A}_f E_t \mathbf{z}_{t+1} + \mathbf{A}_b \mathbf{z}_{t-1} + \mathbf{B}_s \boldsymbol{\varepsilon}_t^s + \mathbf{b}_a \varepsilon_t^a,$$

where \mathbf{A}_0 , \mathbf{A}_b , \mathbf{A}_f , \mathbf{B}_s and \mathbf{b}_a are independent of the skewness of the shocks in ϵ_t^a .

The solution of a linear rational model of the form in eq. [Equation \(1\)](#) can be written as

$$\begin{aligned} \mathbf{z}_t &= \Theta_1 \mathbf{z}_{t-1} + \Theta_0 [\epsilon_t^s \ \epsilon_t^a]' + \Theta_y \sum_{j=1}^{\infty} \Theta_f^{j-1} \Theta_z [E_t \epsilon_{t+j}^s \ E_t \epsilon_{t+j}^a]' \\ &= \Theta_1 \mathbf{z}_{t-1} + \Theta_0 [\epsilon_t^s \ \epsilon_t^a]' + \Theta_y \sum_{j=1}^{\infty} \Theta_f^{j-1} \Theta_z \Xi E_t \epsilon_{t+j}^a. \end{aligned}$$

where the matrices Θ_0 , Θ_1 , Θ_y , and Θ_z are functions of \mathbf{A}_0 , \mathbf{A}_b , \mathbf{A}_f , \mathbf{B}_s and \mathbf{b}_a (see, e.g., [Sims, 2002](#), Sec. 4), whereas Ξ is a selection vector. The last row reflects the fact that $E_t \epsilon_{t+j}^s = \mathbf{0}, \forall j$. In a fully symmetric setting, where $\varrho_{a,t} = 0$ and $E_t \epsilon_{t+j}^a = 0, \forall t, j$, the above expression simplifies to $\mathbf{z}_t = \Theta_1 \mathbf{z}_{t-1} + \Theta_0 [\epsilon_t^s \ \epsilon_t^a]'$. \square

A.3 Macroeconomic effects of revisions in the balance of risk

When shock distributions are skewed, expectations are a function of the asymmetry of the distribution. For the general class of skew-distributions we consider ([Arellano-Valle et al., 2005](#)), the expected value of a generic skew-variate $X \sim f(\mu, \sigma, \varrho)$ takes the form $EX = \mu + \kappa \sigma \varrho$, where μ represents the mode of the distribution, σ captures the dispersion, ϱ summarizes the asymmetry of the distribution about the mode, κ is a constant that depends on the choice of f . Therefor, for $\epsilon_t^a \sim \mathcal{F}(0, \sigma, \varrho_{a,t})$,

$$E_t \epsilon_{t+j}^a = k \sigma^2 E_t \varrho_{a,t+j},$$

such that, when risk evolves over time, shifts in expectations of future asymmetry lead agents to revise their decisions today. Therefore,

$$\mathbf{z}_t = \Theta_1 \mathbf{z}_{t-1} + \Theta_0 [\epsilon_t^s \ \epsilon_t^a]' + \Theta_y \sum_{j=1}^{\infty} \Theta_f^{j-1} \Theta_z \Xi k \sigma^2 E_t \varrho_{a,t+j}.$$

Defining revisions in the asymmetry of risk j periods in advance as $\varrho_t^j = E_t \varrho_{a,t+j} - E_{t-1} \varrho_{a,t+j}$, implies that the h -step ahead impulse response of the system to a revision in the perceived asymmetry

of risk j -periods ahead can be defined as

$$E_t \mathbf{z}_{t+h} - E_{t-1} \mathbf{z}_{t+h} = \mathbf{M}(j, h) k \sigma^2 \varrho_t^j;$$

where $\mathbf{M}(j, h) = \boldsymbol{\Theta}_1^h \boldsymbol{\Theta}_y \boldsymbol{\Theta}_f^{j-1} \boldsymbol{\Theta}_z \boldsymbol{\Xi}$ is a convolution of the system matrices in [Equation \(2\)](#)

A.4 Proof of [Proposition 2](#)

Proof. Let us now consider an alternative model with linear solution given by

$$\mathbf{A}_0 \mathbf{z}_t = \mathbf{A}_f \tilde{E}_t \mathbf{z}_{t+1} + \mathbf{A}_b \mathbf{z}_{t-1} + \mathbf{B} \tilde{\epsilon}_t, \quad (\text{A2})$$

where \tilde{E}_t denotes agents (potentially) distorted beliefs.

In this setting, agents' choices and equilibrium outcomes depend not only on current shocks but also on their beliefs about future shocks. Let \tilde{E}_t denote the *belief expectation* operator, defined as

$$\tilde{E}_t \epsilon_{t+j} = E_t \epsilon_{t+j} + \varphi_{t,t+j}, \quad (\text{A3})$$

where $\varphi_{t,t+j}$ captures agents' beliefs at time t about the mean of the distribution of certain shocks expected to hit the economy at time $t+j$. Under the maintained assumption that the shocks ϵ_t are symmetric—i.e., $E_t \epsilon_{t+1} = \mathbf{0}$ for all t —the term $\varphi_{t,t+j}$ acts as a belief-based adjustment to the expected future shocks.

The solution of a linear rational model of the form in eq. [Equation \(A2\)](#) can be written as

$$\mathbf{z}_t = \boldsymbol{\Theta}_1 \mathbf{z}_{t-1} + \boldsymbol{\Theta}_0 \tilde{\epsilon}_t + \boldsymbol{\Theta}_y \sum_{j=1}^{\infty} \boldsymbol{\Theta}_f^{j-1} \boldsymbol{\Theta}_z \tilde{E}_t \tilde{\epsilon}_{t+j}$$

where the matrices $\boldsymbol{\Theta}_0$, $\boldsymbol{\Theta}_1$, $\boldsymbol{\Theta}_y$, and $\boldsymbol{\Theta}_z$ are functions of \mathbf{A}_0 , \mathbf{A}_b , \mathbf{A}_f , \mathbf{B}_s and \mathbf{b}_a (see, e.g., [Sims, 2002](#), Sec. 4). Therefore, given the definition of *beliefs expectations* in Eq. [\(A3\)](#), the rational

expectations solution of the system can be written as

$$\mathbf{z}_t = \Theta_1 \mathbf{z}_{t-1} + \Theta_0 \tilde{\epsilon}_t + \Theta_y \sum_{j=1}^{\infty} \Theta_f^{j-1} \Theta_z E_t \varphi_{t+j}$$

Let $\varphi_t^j = \varphi_{t,t+j} - \varphi_{t-1,t+j}$ denote a belief revision (or “dummy surprise”), capturing the change between periods $t - 1$ and t in agents’ beliefs about shocks occurring at time $t + j$. Belief distortions evolve as a reflection of agents’ revised views, according to $\varphi_{t,t+h} = \sum_{j=0}^J \varphi_{t-j}^{h+j}$, where J is the maximum horizon over which agents project their distorted expectations. In line with [Chahrour and Jurado \(2018\)](#), we assume that agents do not anticipate future revisions to their beliefs—formally, $E_t \varphi_{t+i}^j = 0$ for all $i \geq 1$.

It follows that revisions in beliefs lead to the following revision of current and expectations of future outcomes:

$$E_t \mathbf{z}_{t+j} - E_{t-1} \mathbf{z}_{t+j} = \Theta_1^j \Theta_y \Theta_f^{j-1} \Theta_z \varphi_t^j, \quad h \geq 0. \quad (\text{A4})$$

By setting

$$\varphi_t^j = \Xi \varphi_t^j = \varkappa \sigma^2 \varrho_{a,t}^j,$$

the impact of revisions about the asymmetry of shocks’ distributions (see [Equation \(4\)](#)) is equivalent to shifts in beliefs about future realizations of the shocks ([Equation \(A4\)](#)) and the responses of the two models are observationally equivalent up the first order. \square

B Solving the New Keynesian model with cost-push shock

In this appendix, we provide detailed derivations of the solutions for the optimal monetary problem under asymmetric risks, outlined in [Section 3](#). This problem is derived in the basic New Keynesian model presented in Chapter 3 of [Galí \(2008\)](#). We briefly outline the households and firms problems, and then derive the optimal monetary policy rules.

B.1 The baseline New Keynesian model

The model features a continuum of households, firms, and a central bank. Households work, consume, and save. Firms hire labor in a competitive market, produce goods, and set prices, with the market for goods being monopolistically competitive. Price setting is subject to the Calvo lottery. Monetary policy is optimal under the assumption that the central bank can commit to future actions. The optimal monetary problem faced by the central bank is discussed in the next section of this appendix.

Households. An infinitely-lived representative agent seeks to maximize

$$E_0 \sum_{t=0}^{\infty} \beta^t U(C_t, N_t),$$

subject to the budget constraint

$$P_t C_t + Q_t B_t \leq B_{t-1} + W_t N_t + T_t, \text{ for } t = 1, 2, \dots,$$

where C_t and P_t represent the quantity and price of the aggregate consumption index, Q_t is the price of a nominal bond purchased in quantity B_t , N_t denotes the hours worked, remunerated at the nominal wage W_t ; finally, T_t is a lump-sum transfer. There is a CES technology aggregating differentiated goods produced by firms into the consumption bundle, C_t , consumed by the representative household. The parameter β is the deterministic discount factor of households.

Assuming the utility function to be

$$U(C_t, N_t) = \frac{C_t^{1-\sigma}}{1-\sigma} - \frac{N_t^{1-\varphi}}{1-\varphi},$$

where σ is the parameter of relative risk aversion and φ is the inverse Frisch elasticity of labor supply. Households' demand for a differentiated good is downward sloping with respect to the price of the good.

Firms. A continuum of monopolistic firms produce differentiated goods using the same technology

$$Y_t(i) = A_t N_t(i)^{1-\alpha},$$

where A_t denotes the technology level, and α is the production function scale parameter. All firms face the same downward-sloping demand schedule obtained from solving the household's problem of choosing goods of different variety.

We assume that, every period, a firm can re-optimize its prices with probability $1 - \theta$. This friction gives rise to the following dynamics for the aggregate price level, expressed in log-terms,

$$\pi_t = (1 - \theta)(p_t^* - p_{t-1}),$$

where p_t^* is the re-optimized price level and p_{t-1} is the average price level for the non-re-optimizing firms.

B.2 The optimal monetary policy problem

In this model, the output gap and inflation in deviations from steady state are governed by a standard IS and a Phillips curve

$$\hat{x}_t = E_t \hat{x}_{t+1} - \frac{1}{\sigma} \left(\hat{i}_t + E_t \hat{\pi}_{t+1} \right), \quad (\text{B1})$$

$$\hat{\pi}_t = \beta E_t \pi_{t+1} + \kappa \hat{x}_t + u_t, \quad (\text{B2})$$

where $i_t = -\log Q_t$ is the short-term nominal rate and κ is the slope of the Phillips curve. To simplify the exposition, we assume that cost-push shocks follow $u_t \sim \text{i.i.d. } \mathcal{N}(0, \sigma_u)$.²⁵

We assume that the central bank commits, with full credibility, to a policy plan consistent with a quadratic objective function in inflation deviations, $\hat{\pi}_t$ and the output gap, \hat{x}_t . Therefore,

²⁵Although we adopt the standard normality assumption, the results only require that the shock is univariate and symmetric. In this case, the mean and the central forecast coincide, implying $E_t u_{t+j} = 0$ for all $j \geq 1$, which is sufficient to derive the solution under symmetry.

optimal monetary policy consists in choosing the state-contingent $\{\hat{\pi}_t, \hat{x}_t\}_{t=0}^{\infty}$ that minimizes

$$\frac{1}{2}E_0 \sum_{t=0}^{\infty} \beta^t (\hat{\pi}_t^2 + \alpha_x \hat{x}_t^2),$$

subject to the sequence of constraints imposed by the Phillips curve above. Casting the problem into its Lagrangian form

$$\mathcal{L} = E_0 \sum_{t=0}^{\infty} \beta^t \left[\frac{1}{2} (\hat{\pi}_t^2 + \alpha_x \hat{x}_t^2) + \gamma_t (\hat{\pi}_t - \kappa \hat{x}_t - \beta \hat{\pi}_{t+1}) \right],$$

and differentiating with respect to \hat{x}_t and $\hat{\pi}_t$ yields the optimality conditions

$$\alpha_x \hat{x}_t - \kappa \gamma_t = 0$$

$$\hat{\pi}_t + \gamma_t - \gamma_{t-1} = 0$$

that must hold for $t = 0, 1, 2, \dots$; We set $\gamma_{-1} = 0$ in that Phillips curve constraint is not binding in period -1 for the central bank choosing the optimal plan in period 0.

Standard manipulations yield the following optimality conditions,

$$\begin{aligned} \hat{x}_0 &= -\frac{\kappa}{\alpha_x} \hat{\pi}_0, \\ \hat{x}_t &= \hat{x}_{t-1} - \frac{\kappa}{\alpha_x} \hat{\pi}_t, \quad \forall t. \end{aligned}$$

Define $\bar{p}_t = p_t - p_{-1}$ as the inflation rate over period 0 through period t , where p_t denotes the log of the price level at time t . We can now write the optimal targeting rule under commitment as

$$\hat{x}_t = -\frac{\kappa}{\alpha_x} \bar{p}_t, \tag{B3}$$

such that the optimizing central bank keeps output below or above the efficient level in proportion to the deviations of the price level from its implicit target. Plugging [Equation \(B3\)](#) into

Equation (B2) we can recast the Phillips curve in as

$$\bar{p}_t = a\bar{p}_{t-1} + a\beta E_t \bar{p}_{t+1} + au_t \quad (\text{B4})$$

with $a \equiv \frac{\alpha_x}{\alpha_x(1+\beta)+\kappa^2}$.

B.2.1 The symmetric case

The stationary solution to Equation (B4) can be obtained by using the method of undetermined coefficients by conjecturing a solution of the form

$$\bar{p}_t = \eta\bar{p}_{t-1} + \lambda u_t, \quad (\text{B5})$$

such that the expected value of the next period's price level is

$$E_t \bar{p}_{t+1} = \eta\bar{p}_t. \quad (\text{B6})$$

Substituting the expectations implied by the stationary solution yields

$$\begin{aligned} \bar{p}_t &= a\bar{p}_{t-1} + a\beta\eta\bar{p}_t + au_t \\ \bar{p}_t &= \underbrace{\frac{a}{1-a\beta\eta}}_{\eta} \bar{p}_{t-1} + \underbrace{a\frac{1}{1-a\beta\eta}}_{\lambda} u_t \end{aligned}$$

Solving for η and λ , we obtain

$$\eta = \frac{1 - \sqrt{1 - 4\beta a^2}}{2a\beta}, \quad (\text{B7})$$

$$\lambda = \frac{a}{1 - a\beta\eta}, \quad (\text{B8})$$

and we can express the equilibrium process for the output gap as

$$\hat{x}_t = \eta\hat{x}_{t-1} - \frac{\kappa}{\alpha_x}\lambda u_t, \quad (\text{B9})$$

for $t = 1, 2, \dots$, with $\hat{x}_0 = -\frac{\kappa}{\alpha_x} \lambda u_0$.

Implementation. The optimality condition in Equation (B3) allows us to write the IS curve in Equation (B1) as

$$\left[1 - \sigma \frac{\kappa}{\alpha_x}\right] \bar{p}_t = \left[1 - \sigma \frac{\kappa}{\alpha_x}\right] E_t \bar{p}_{t+1} - \hat{i}_t.$$

Now, substituting the implied expectation derived in Equation (B6), we obtain the following *optimal monetary rule*:

$$\hat{i}_t = -(1 - \eta) \left[1 - \sigma \frac{\kappa}{\alpha_x}\right] \bar{p}_t. \quad (\text{B10})$$

Provided that $\phi_p > 0$, the system of equations comprising the IS equation, the Phillips curve, and the optimal monetary rule in the above specification admits a unique stable rational expectations equilibrium (see, e.g., Galí, 2008).

B.2.2 The asymmetric case

Let us now consider the case where the stochastic process driving the cost-push shock is no longer symmetric. Specifically, assume that the shocks follow $\tilde{u}_t \sim \text{i.i.d. } f(0, \sigma_u, \varrho_{u,t})$, where $f(0, \sigma_u, \varrho_{u,t})$ denotes a general unimodal distribution centered at zero but asymmetric when $\varrho_{u,t} \neq 0$. In this setting, the perceived risk associated with the distribution evolves over time as agents update their views about the balance of upside and downside risks. As a result, the expected value of future shocks reflects these changes in perceived asymmetry. While the mode—the most likely outcome—remains at zero, the mean shifts with the asymmetry, so that $E_t \tilde{u}_{t+j} = \varkappa \sigma_u E_t \varrho_{u,t+j}$.

To simplify the characterization of optimal monetary policy, we assume that agents receive news about the skewness of the distribution only up to $J = 1$ period ahead. Beyond that, they assume all risk is symmetric. In this environment, at time t , agents observe the current realization of the shock and form expectations about future realizations based on their current perception of asymmetry. This implies $E_t \tilde{u}_{t+1} = \varkappa \sigma_u E_t \varrho_{u,t+1}$, while $E_t \tilde{u}_{t+j} = 0$ for all $j > 1$. Moreover,

since $\varrho_{u,t+1} = \varrho_{u,t+1}^0 + \varrho_{u,t}^1$, and assuming agents do not anticipate further revisions in perceived asymmetry (i.e., $E_t \varrho_{u,t+1}^0 = 0$), it follows that $E_t \tilde{u}_{t+1} = \varkappa \sigma_u \varrho_{u,t}^1$, where $\varrho_{u,t}^1 = E_t \varrho_{u,t+1} - E_{t-1} \varrho_{u,t+1}$. Expectations of future shocks therefore reflect the latest update in perceived risk asymmetry.

We now turn to the alternative *beliefs representation* of the information structure. In this framework, agents observe the realization of the shock at time t and update their beliefs about both the current shock, denoted by ψ_t^0 , and the next period's shock, denoted by ψ_t^1 . These belief distortions are mapped into expectations as follows:

$$E_t \tilde{u}_t = u_t + \psi_t^0 + \psi_{t-1}^1 = \tilde{u}_t, \quad (\text{B11})$$

$$E_t \tilde{u}_{t+1} = E_t \psi_{t+1}^0 + \psi_t^1 = \psi_t^1. \quad (\text{B12})$$

Equation (B11) imposes the restriction $\psi_t^0 = -\psi_{t-1}^1$, requiring that the actual realization of the shock is not affected by prior beliefs—or equivalently, that earlier beliefs do not necessarily materialize and can turn out to be pure noise. Equation (B12) reflects the assumption that agents' expectations about future shocks are fully captured by the dummy belief ψ_t^1 , and that they do not anticipate further updates in those beliefs, i.e., $E_t \psi_{t+1}^0 = 0$. Furthermore, by setting $\psi_t^1 = \varkappa \sigma_u \varrho_{u,t}^1$, we have that, up to a first-order approximation, the dynamics of a model with evolving perceptions of asymmetric risk can be equivalently represented by a model with symmetric shocks and belief distortions captured by dummy surprises.

In this setting, shifts in asymmetric risk affect current allocations and as a consequence next period's price level, $E_t \bar{p}_{t+1}$, are potentially distorted. We postulate that the price process under optimal policy evolves as:

$$\bar{p}_t = \eta \bar{p}_{t-1} + \lambda u_t + \zeta \psi_t^1, \quad (\text{B13})$$

and, since $E_t u_{t+1} = \psi_t^1$ and $E_t \psi_{t+1}^1 = 0$, it follows that

$$E_t \bar{p}_{t+1} = \eta \bar{p}_t + \lambda \psi_t^1.$$

Substituting the expectations implied by the stationary solution under optimal policy (Equation (B4)) yields

$$\begin{aligned}\bar{p}_t &= a\bar{p}_{t-1} + a\beta [\eta\bar{p}_t + \lambda\psi_t^1] + au_t, \\ \bar{p}_t &= \underbrace{\frac{a}{1-a\beta\eta}}_{\eta} \bar{p}_{t-1} + \underbrace{\frac{a}{1-a\beta\eta}}_{\lambda} u_t + \underbrace{\frac{a\beta\lambda}{1-a\beta\eta}}_{\zeta} \psi_t^1.\end{aligned}$$

Solving for η , λ and ζ we obtain

$$\begin{aligned}\eta &= \frac{1 - \sqrt{1 - 4\beta a^2}}{2a\beta}, \\ \lambda &= \frac{a}{1 - a\beta\eta}, \\ \zeta &= \frac{a\beta\lambda}{1 - a\beta\eta}.\end{aligned}$$

Since under optimal policy $\hat{x}_t = -\frac{\kappa}{\alpha_x}\bar{p}_t$, the equilibrium process for the output gap reads as

$$\hat{x}_t = \eta\hat{x}_{t-1} - \frac{\kappa}{\alpha_x} [\lambda u_t + \zeta\psi_t^1], \quad (\text{B14})$$

and $\hat{x}_0 = -\frac{\kappa}{\alpha_x} [\lambda u_0 + \zeta\psi_0^1]$.

Implementation. Let us rewrite the IS equation in terms of the price level under asymmetry and substitute the optimality condition such that

$$\left[1 - \sigma \frac{\kappa}{\alpha_x}\right] \bar{p}_t = \left[1 - \sigma \frac{\kappa}{\alpha_x}\right] E_t \bar{p}_{t+1} - \hat{i}_t.$$

Substituting the expectation for the price level under asymmetry, we obtain the *optimal monetary rule under asymmetry*:

$$\hat{i}_t = -(1 - \eta) \left[1 - \sigma \frac{\kappa}{\alpha_x}\right] \bar{p}_t + \left[1 - \sigma \frac{\kappa}{\alpha_x}\right] \lambda \psi_t^1, \quad (\text{B15})$$

where the first term in the right-hand side is the same as in Equation (B10), and the last term captures how the central bank must adjust the policy rate in response to shifts in perceived risk asymmetry, specifically accounting for how these changes influence agents' expectations.²⁶

B.2.3 Asymmetric case with an unwitting central bank

We now consider the case in which the distribution of cost-push shocks are skewed but the central bank does not take this into account (or it does not know) and adopts the optimal policy under the incorrect assumption about shocks distributions. This exercise can be also interpreted as the asymmetric case under the counterfactual assumption that the central bank does not try to lean against the asymmetry in the dynamics of the price level.

We start from the optimality condition between output gap and inflation

$$\hat{x}_t = -\frac{\kappa}{\alpha_x} \bar{p}_t^m, \quad (\text{B16})$$

where \bar{p}_t^m is the (mispecified) price level the central bank is targeting, under the incorrect perception that of symmetric risk, i.e. under the assumption that $\psi_t^j = 0, \forall t, j$. This *mispecified* price level evolves according to

$$\bar{p}_t^m = \eta \bar{p}_{t-1} + \lambda u_t. \quad (\text{B17})$$

Note that this is not exactly the same price level as in fully symmetric case, because prices (\bar{p}_t) are affected by agents' beliefs of skewed risk. To see that, write the Phillips curve in terms of the price level,

$$(1 + \beta) \bar{p}_t = \bar{p}_{t-1} + \kappa \hat{x}_t + \beta E_t \bar{p}_{t+1} + u_t,$$

and conjecture that the difference between the actual prices and the prices that the central bank

²⁶It can be shown that the conditions for determinacy are the same as in the model with symmetric risk.

incorrectly targets when solving the optimal problem takes the form

$$\bar{p}_t - \bar{p}_t^m = \tau \psi_t^1.$$

By plugging this equation into the optimality condition in [Equation \(B16\)](#), and substituting into the Phillips curve expressed in terms of price level yields

$$\bar{p}_t = a\bar{p}_{t-1} + a\beta E_t \bar{p}_{t+1} + b\tau \psi_t^1 + au_t \quad (\text{B18})$$

with $a \equiv \frac{\alpha_x}{\alpha_x(1+\beta)+\kappa^2}$ and $b \equiv \frac{\kappa^2}{\alpha_x(1+\beta)+\kappa^2}$.

As before, we conjecture the stationary solution, retrieve expectations of next period's price level and plug these into [Equation \(B18\)](#) to obtain

$$\bar{p}_t = \underbrace{\frac{a}{1-a\beta\eta}}_{\eta} \bar{p}_{t-1} + \underbrace{\frac{a}{1-a\beta\eta}}_{\lambda} u_t + \underbrace{\frac{a\beta\lambda+b\tau}{1-a\beta\eta}}_{\tilde{\zeta}} \psi_t^1. \quad (\text{B19})$$

Solving for the coefficients we obtain

$$\begin{aligned} \eta &= \frac{1 - \sqrt{1 - 4\beta a^2}}{2a\beta} \\ \lambda &= \frac{a}{1 - a\beta\eta} \\ \tilde{\zeta} &= \frac{a\beta\lambda + b\tau}{1 - a\beta\eta} \end{aligned}$$

Comparing [Equation \(B19\)](#) with [Equation \(B13\)](#), note that the misspecified policy reaction implies $\tilde{\zeta} > \zeta$. As a result, by failing to respond to shifts in the asymmetry of risk, the central bank amplifies the sensitivity of inflation to those shifts.

We recover τ by taking the difference between the price level, \bar{p} , and the price level under the symmetric policy – [Equation \(B17\)](#). Specifically,

$$\bar{p}_t - \bar{p}_t^m = \underbrace{\frac{a\beta\lambda + b\tau}{1 - a\beta\eta}}_{\tau} \psi_t^1,$$

which leads to

$$\tilde{\zeta} = \tau = \frac{a\beta\lambda}{1 - a\beta\eta - b}. \quad (\text{B20})$$

It should be noted that a central bank that overlooks the role of imbalanced risks will end up setting the output gap as a function of \bar{p}_t^m . However, this price level is not attainable due to the presence of asymmetric inflation risks. As a result, the central bank achieves a suboptimal output gap and a realized price level that deviates from its target, \bar{p}_t^m .

Under the optimal policy, the equilibrium process for the output gap is given by $\hat{x}_t = -\frac{\kappa}{\alpha_x}\bar{p}_t^m$, for all t . Therefore, in the first period, $\hat{x}_0 = -\lambda\frac{\kappa}{\alpha_x}u_t$. That is, the central bank's response in the initial period—while ignoring the effects of skewed risk—results in an output gap equal to that under symmetric risk. This occurs because, in the first period, the price level targeted by the central bank, \bar{p}_t^m , coincides with the price level targeted by a central bank assuming symmetric risk.²⁷ However, in subsequent periods, the output gap begins to diverge across the two economies as the prior period's price level differs due to the skewness in the shock distribution. Specifically, with an unwitting central bank:

$$\hat{x}_t = \eta\hat{x}_{t-1} - \frac{\kappa}{\alpha_x} \left[\lambda u_t + \tilde{\zeta}\eta\psi_{t-1}^1 \right].$$

B.3 Calibration values for the numerical simulation

We follow Galí (2008) and set the following values for the parameters of the model: the elasticity of substitution, σ , to unity, the production function scale parameter, α , is set to one third, the elasticity of substitution among intermediate goods, ε , is equal to 6, and the slope of the Phillips curve, κ , is equal to 0.1275.

²⁷We assume that in period $t = -1$, the economy is at the deterministic steady-state equilibrium where risks are fully balanced, $\psi_{-i}^i = 0$, for $i = -1, -2, \dots$

Table C1: Time variation in higher order moments

	Q	Q^*	N	Q	Q^*	N
	<i>Homoskedastic</i>			<i>Heteroskedastic</i>		
<i>Scale</i> ²				369.36***	373.67***	1.50***
<i>Asymmetry</i>	367.31***	371.60***	4.18***	35.65***	36.07***	0.79***

Note: Q is the portmanteau test, Q^* is the Ljung-Box extension (with automatic lag selection) and N corresponds to the Nyblom test. Q and Q^* are distributed as a χ_1^2 , while N is distributed as a Cramer von-Mises distribution with 1 degree of freedom. * $p < 10\%$, ** $p < 5\%$, *** $p < 1\%$.

C Inflation risk: additional results

This appendix reports additional details and results to complement what reported in [Section 4](#).

C.1 Formally testing for inflation conditional skewness

We formally test for the evidence of time variation in the asymmetry of the predictive distributions of core PCE inflation. Assuming a flexible Skew- t specification for the likelihood function of inflation data, we test whether the asymmetry of the conditional distribution can be significantly assumed to be constant by examining the properties of the score function. [Table C1](#) reports the results of three alternative parametric Lagrange Multiplier tests: a Q test, an adjusted Q^* test, and the Nyblom test, following [Delle Monache et al. \(2024\)](#).²⁸ All test strongly reject the null hypothesis of symmetry at the 1% confidence level; the right panel of the Table show an equally strong rejection after accounting for stochastic volatility. Similar results are obtained by applying [Bai and Ng \(2005\)](#) tests for unconditional skewness to an expanding window of data, as reported in [Figure C1](#).

C.2 The model

Let $\pi_t = 400 \log(p_t/p_{t-1})$ denote the annualized, quarter-on-quarter (core) PCE inflation rate, and assume that at each point in time the distribution of π_t can be characterized by a Skew- t

²⁸These tests consist of fitting the data to a *Skew- t* distribution, defined by parameters of location, scale and asymmetry. A score-based test can then be used to test for the stability of the fixed parameters. We also account for the possibility of fat tails in the distribution (see [Harvey and Thiele, 2016](#); [De Polis, 2023](#)).

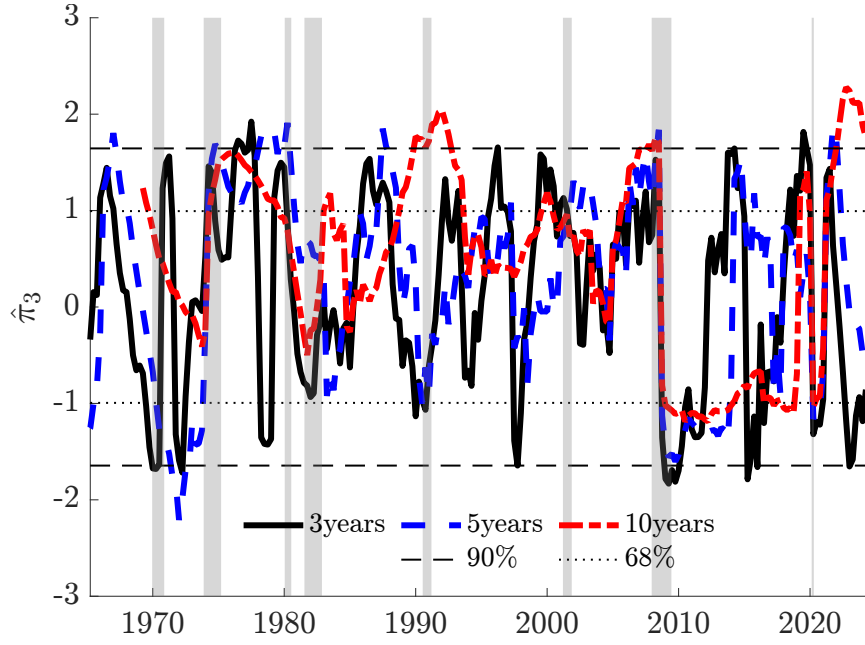


Figure C1: Bai and Ng (2005) rolling tests

Note: The figure reports rolling Bai and Ng (2005) test statistics for US core PCE, using windows of 3, 5 and 10 years, and the the 68 and 90% critical values.

Table C2: Parameters estimates for the econometric model in [Section 4](#)

Autocorrelations					
ϕ_μ	ϕ_γ	ϕ_δ			
0.989 (0.007)	0.866 (0.058)	0.834 (0.062)			
Learning rates					
a_μ	b_μ	a_γ	b_γ	a_δ	b_δ
0.092 (0.007)	0.095 (0.005)	0.043 (0.019)	0.087 (0.010)	0.024 (0.012)	0.079 (0.016)
Degrees of freedom					
η					
0.141 (0.037)					

Note: The table reports mean estimates of the static parameters of the model. Parameters standard deviations are reported in parentheses.

(Sk_t) distribution with time-varying location (μ_t), scale (σ_t), and shape (ϱ_t) parameters:

$$\pi_t \sim Skt_\nu(\mu_t, \sigma_t^2, \varrho_t),$$

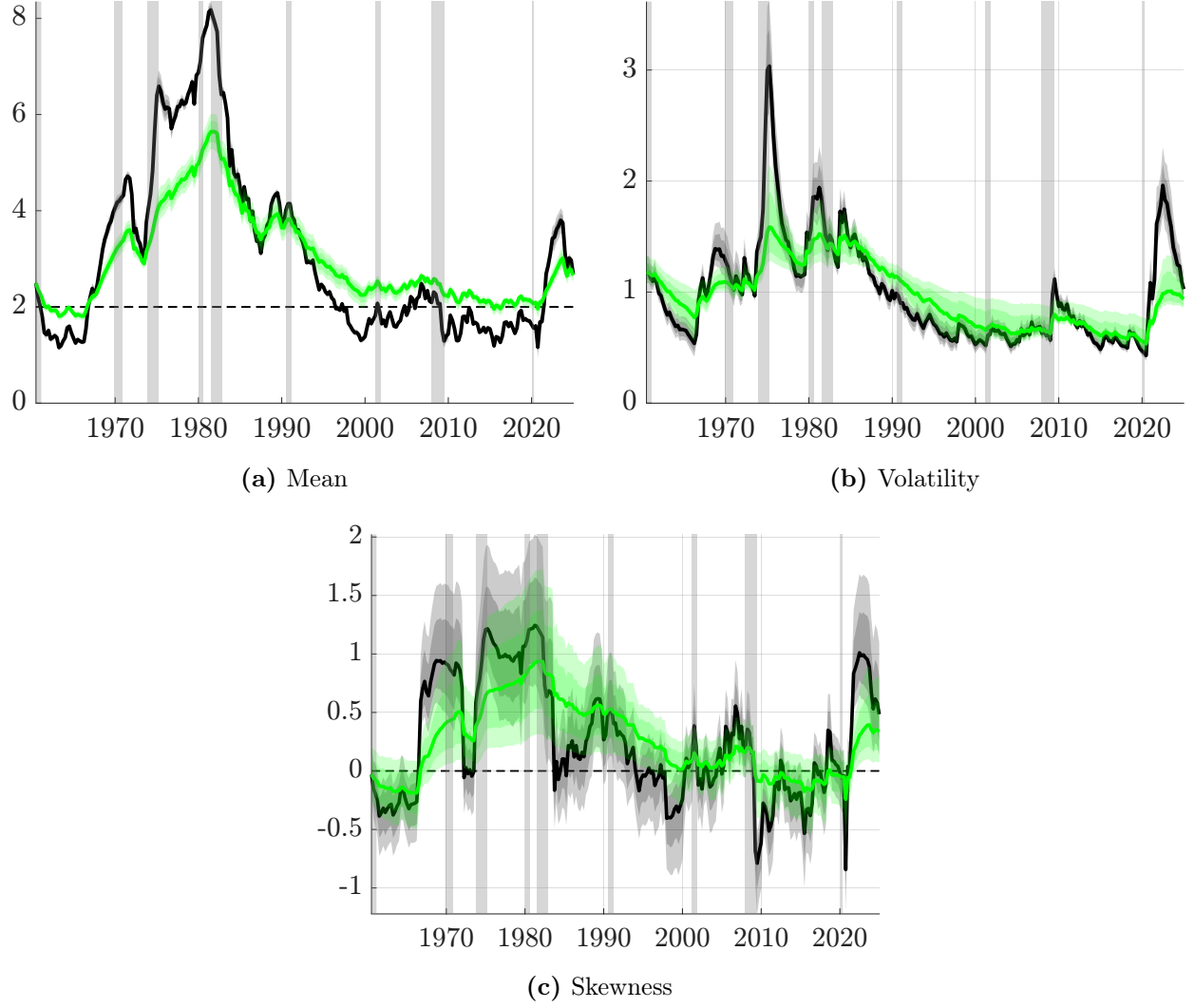


Figure C2: Time-varying moments of core PCE in the US

Note: The panels report mean, volatility and skewness of US core PCE. Black lines represent total moments, green lines correspond to long-run components only. Bands report 68 and 96% credible intervals. Gray shaded areas represent NBER recessions.

where ν denotes the, time invariant, degrees of freedom. The degree of the asymmetry is risk is captured by the parameter $\varrho_t \in (-1, 1)$. We postulate that each parameter features a permanent and transitory component, such that the location is

$$\mu_t = \bar{\mu}_t + \tilde{\mu}_t \tag{C1}$$

$$\bar{\mu}_t = \bar{\mu}_t + a_\mu s_{\mu,t} \tag{C2}$$

$$\tilde{\mu}_t = \phi_\mu \tilde{\mu}_t + b_\mu s_{\mu,t}. \tag{C3}$$

Let $\delta_t = \log(\sigma_t)$, then

$$\gamma_t = \bar{\gamma}_t + \tilde{\gamma}_t \quad (\text{C4})$$

$$\bar{\gamma}_t = \bar{\gamma}_t + a_\gamma s_{\gamma,t} \quad (\text{C5})$$

$$\tilde{\gamma}_t = \phi_\gamma \tilde{\gamma}_t + b_\gamma s_{\gamma,t}, \quad (\text{C6})$$

such that the scale parameter is multiplicative in its two components. Finally, for $\gamma_t = \text{arctanh}(\varrho_t)$ we have

$$\delta_t = \bar{\delta}_t + \tilde{\delta}_t \quad (\text{C7})$$

$$\bar{\delta}_t = \bar{\delta}_t + a_\delta s_{\delta,t} \quad (\text{C8})$$

$$\tilde{\delta}_t = \phi_\delta \tilde{\delta}_t + b_\delta s_{\delta,t}. \quad (\text{C9})$$

More compactly, for $f_t = (\mu_t, \delta_t, \gamma_t)'$,

$$\bar{f}_{i,t} = \bar{f}_{i,t-1} + a_i s_{i,t-1}, \quad (\text{C10})$$

$$\tilde{f}_{i,t} = \phi_i \tilde{f}_{i,t-1} + b_i s_{i,t-1}. \quad (\text{C11})$$

The time-varying parameters of the distribution are learned in real-time, with updates being proportional to $s_{i,t-1}$, which is the *scaled score* of the conditional distribution (as in [Creal et al., 2013](#); [Harvey, 2013](#)). Refer to [Appendix D](#) for derivations of the scaled scores and the estimation procedure.

C.3 Additional estimation results

The estimated time-varying moments of core PCE are reported in [Figure C2](#), where we highlight the permanent components and the total moment in green and black, respectively. Specifically, moments are closed-form functions of the estimated time-varying parameters.

$$E_{t-1}\pi_t = \mu_t + \underbrace{g(\eta)\sigma_t\varrho_t}_{\psi_t}, \quad g(\eta) = \frac{4\mathcal{C}(\eta)}{1-\eta}, \quad (\text{C12})$$

$$Var_{t-1}\pi_t = \sigma_t^2 \left(\frac{1}{1-2\eta} + h(\eta)\varrho_t^2 \right), \quad h(\eta) = \frac{3}{1-2\eta} - g(\eta)^2, \quad (\text{C13})$$

$$Skew_{t-1}\pi_t = \frac{g(\eta)\varrho_t [1 + \eta - \varrho_t^2 (5 - 2g(\eta)^2 + (10g(\eta)^2 - 19)\eta - 12g(\eta)^2\eta^2)]}{(1-3\eta)(1-2\eta) \left(\frac{1}{1-2\eta} + h(\eta)\varrho_t^2 \right)^{\frac{3}{2}}}, \quad (\text{C14})$$

noting that this moment only depends on the asymmetry parameter and on the estimated degrees of freedom (see [De Polis, 2023](#)).

We also report in [Table C2](#) the estimated static parameters of the model, which consists of three autoregressive parameters for the transitory components, six learning rates for the pair of components of the time-varying parameters, and the fixed (inverse of the) degrees of freedom on the distribution.

C.4 Additional forecasting results

Table C3: Out-of-sample comparison - *Student t*

	h = 1	h = 2	h = 3	h = 4	h = 8
MSFE	0.865 (0.000)	0.901 (0.000)	0.926 (0.000)	0.970 (0.000)	1.006 (0.939)
CRPS	0.957 (0.001)	0.970 (0.000)	0.969 (0.000)	0.980 (0.006)	0.995 (0.066)
CRPS decomposition					
Right	0.945 (0.000)	0.945 (0.000)	0.952 (0.000)	0.966 (0.000)	0.985 (0.002)
Left	0.966 (0.000)	0.991 (0.142)	0.983 (0.006)	0.993 (0.146)	1.004 (0.913)
Center	0.959 (0.001)	0.975 (0.008)	0.972 (0.000)	0.984 (0.007)	0.997 (0.147)

Note: The table report the relative performance of a t model against our Skew- t model. Results are reported in ratios, with our model being at the numerator; values smaller than 1 imply superior predictive accuracy of the Skew- t model. The out-of-sample period runs from 2000Q1 to 2024Q2. Values in **bold** are significant at the 10% level.

Table C4: Event forecast comparison against SPF

	$\pi_t^{Q4} < 1.5\%$				$1.5\% \leq \pi_t^{Q4} \leq 2.5\%$				$\pi_t^{Q4} > 2.5\%$			
	h = 1	h = 2	h = 3	h = 4	h = 1	h = 2	h = 3	h = 4	h = 1	h = 2	h = 3	h = 4
SPF	1.216	0.929	1.217	0.890	1.118	0.928	1.376	1.120	0.910	0.235	0.530	0.847
UCSV	0.998	1.063	1.023	0.995	1.053	1.033	1.031	0.984	0.917	0.738	0.831	0.838

Note: The table reports the ratio of the Brier score of SPF and UCSV over our Skew- t model event predictions. The target variable is Q4-over-Q4 core PCE. The evaluation sample runs from 2007Q1 due to SPF data availability.

C.5 Bayesian estimation

Posterior estimates of the parameters are obtained via simulation by means of an Adaptive Metropolis-Hastings algorithm (Haario et al., 1999). Given that estimated parameters lie in bounded regions of the parameter space, we augment the algorithm with a rejection step to prevent numerical instability due to invalid parameter draws.

- (i) Sample θ^j from a random walk candidate density;
- (ii) Reject draws that do not respect parameter bounds;
- (iii) Compute $\{f_1, \dots, f_T|\theta^j\}$, the log-likelihood $\ell(y|\theta^j)$, and the posterior $\pi(\theta^j|y)$;
- (iv) Accept or reject θ^j according to the MH rule and update the sampling variance;
- (v) To improve the convergence of the algorithm, we allow for delayed acceptance in case a draw gets rejected (see, e.g., Sherlock et al., 2017).
- (vi) Compute the statistics of interest as the percentiles of the empirical distribution function.

The algorithm is rather efficient, and a complete chain of 50000 draws can be obtained in about 2 minutes. Section D in Delle Monache et al. (2024) provides detailed explanation of the algorithm.

C.5.1 Priors

The initial values for the permanent component of time-varying parameters are drawn from a multivariate Gaussian distribution, $\bar{f}_0 \sim \mathcal{N}(\mathbf{m}_0, \mathbf{s}_0)$, with mean vector \mathbf{m}_0 and covariance matrix \mathbf{s}_0 . The mean vector is fixed to $[2.5 \ 0 \ 0]'$, which captures the properties of the first ten years of

data. The covariance matrix is computed as $\mathbf{s}_0 = E[\nabla'_{\mathbf{g}_0} \nabla_{\mathbf{g}_0}]^{-1}$, where $\nabla_{\mathbf{m}_0} = \frac{\partial \mathbf{g}_0}{\partial \mathbf{m}_{0,j}}$ is the gradient of \mathbf{g}_0 , a function matching sample moments to the three parameters of interest. We use Minnesota-type priors for the persistence of the transitory components, $\phi \sim NID(\mu_\phi, \sigma_\phi) \cdot I_{(\phi \in \Phi)}$. We target high persistence, with $\mu_\phi \lesssim 1$, with a standard tightness of $\sigma_\mu = 0.2$, in line with Bayesian Vector Autoregressive models (see, e.g., [Doan et al., 1984](#); [Sims and Zha, 1998](#)). We restrict the prior distribution to only span the stationary region, Φ , by truncating the support, which gives rise to an improper prior distribution as in [Cogley and Sargent \(2005\)](#). Loadings on the score components are Gamma distributed with shape parameter equal to 2 and the scale parameters are set to obtain mean and standard deviation equal to 0.015 and 0.01 for the permanent loadings, a , and 0.07 and 0.05 for the transitory loadings, b . These hyperparameter values correspond to an a-priori half-life of 10 and 2 years for the two components, reflecting the view that transitory parameters are slower to react to news compared to the transitory components. Furthermore, the prior ensures that the filter is invertible ([Blasques et al., 2022](#)), that is it reduces the possibility of overshooting the updates in the direction of the (local) optimum, and assumes conservative views on parameters time variation. Lastly, we assume a gamma prior for ν , ensuring $\nu > 3$, $\nu \sim \mathcal{G}(2, 10) \cdot I_{(\eta \in \mathcal{H})}$.

C.5.2 MCMC Convergence Diagnostics

We consider three types of diagnostics: the graphical inspection of cumulative means, the analysis of variance of several chains, and a test on the ergodic averages. In these exercises we check the convergence of the post burn-in sample, Θ^* , for our preferred model specification. We draw $N = 30000$ replications and we keep the last $n^* = 3000$ replications, after thinning each two posterior draws to reduce the autocorrelation of the chains.

As a first step, we inspect the cumulative averages of the retained draws. A smooth and stable plot suggests that the chain has converged to the expected value of its invariant distribution. The cumulative averages plotted in [Figure C3](#) appear all smooth and converging to the single value $\mathbb{E}[\Theta^*]$, suggesting that the chains have reached convergence.

Next, we turn to analysis of variance techniques, as advocated by [Gelman and Rubin \(1992\)](#).

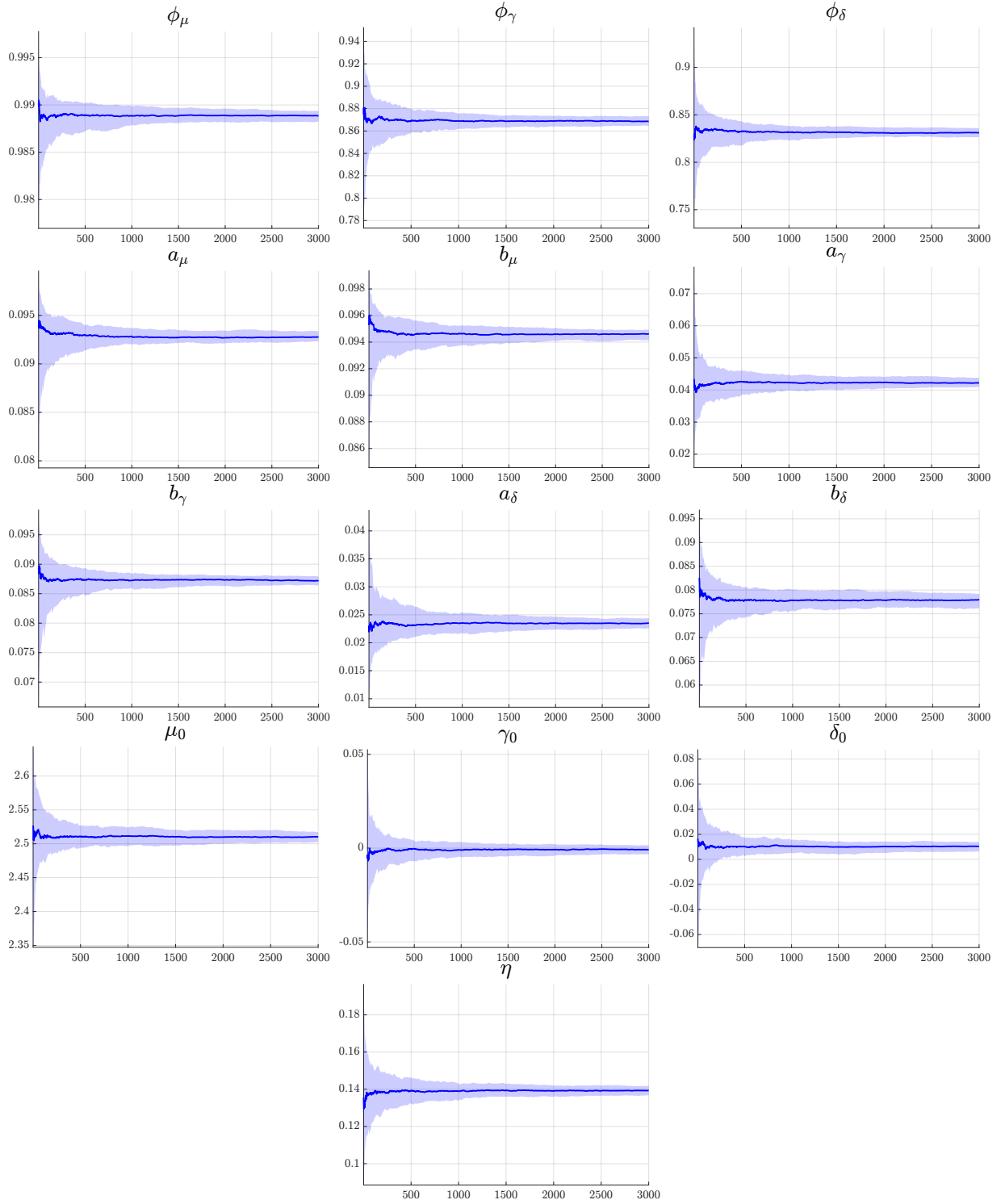


Figure C3: Cumulative averages

Note: The panels show the cumulative averages of the post burn-in sample. ϕ s are the autoregressive parameters, a s and b s are the learning rate parameters for the transitory and permanent components, respectively, μ_0 , γ_0 and δ_0 are the initial values of the permanent components and η is the inverse of the degrees of freedom.

Due to the efficiency of our algorithm, we consider $m = 100$ parallel chains to compare the dispersion *between*, B , and *within*, W , chains, and test that the former is greater than the latter.

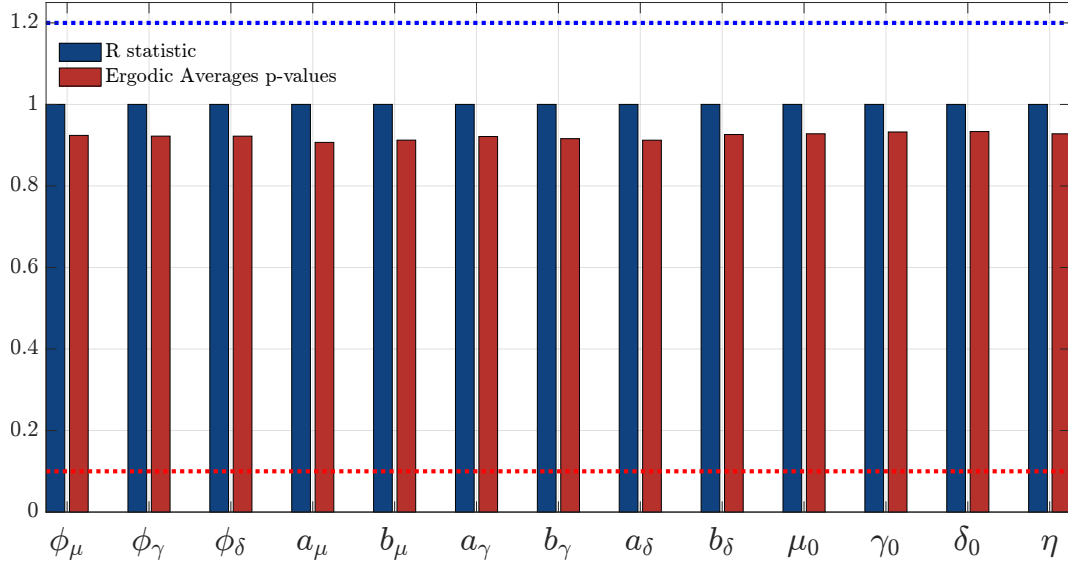


Figure C4: R statistic and ergodic average p-values

Note: The bars represent [Gelman and Rubin \(1992\)](#) R statistic (blue) and the p-values for [Geweke \(1992\)](#) test on ergodic averages (red) for each parameter of the model. The blue dotted line represents the critical value of 1.2 for the R statistics; the red dotted line represents the 10% critical value for the p-values. The statistics are computed for $J=13$ parameters and $m=100$ chains.

Specifically,

$$B = \frac{n^*}{m-1} \sum_{i=1}^m (\bar{\theta}_i^* - \bar{\theta}^*)^2 \quad \text{and} \quad W = \frac{1}{m(n^* - 1)} \sum_{i=1}^m \sum_{j=1}^J (\theta_{i,j}^* - \bar{\theta}_i^*)^2,$$

where $\bar{\theta}_i^* = \frac{1}{n^*} \sum_{n=1}^{n^*} \theta_n^*$ and $\bar{\theta}^* = \sum_{i=1}^m \bar{\theta}_i^*$. These statistics are used to consistently estimate the marginal posterior variance of θ^* as the weighted average of W and B as:

$$\hat{\sigma}_{\theta^*}^2 = \frac{n-1}{n} W + \frac{1}{n} B.$$

Convergence can thus be monitored by means of $\hat{R} = \sqrt{\hat{\sigma}_{\theta^*}^2 W^{-1}} \geq 1$; [Gelman \(1995\)](#) suggest that $R < 1.2$ can be used as an indication to accept the convergence of the MCMC.

At last, we follow [Geweke \(1992\)](#) and test the ergodic averages of the time series of draws. We split the n^* draws into a subsample B of $n_b^* = 0.1n^*$ and another one A of $n_a^* = 0.5n^*$, and compute

$$\bar{\theta}_b^* = \frac{1}{n_b^*} \sum_{j=1}^{n_b^*} \theta_j^* \quad \text{and} \quad \bar{\theta}_a^* = \frac{1}{n_a^*} \sum_{j=n_a^*}^{n^*} \theta_j^*.$$

As we only consider the post burn-in sample, $\bar{\theta}_b^*$ and $\bar{\theta}_a^*$ are the ergodic averages at the beginning and at the end of the convergence sample, and should therefore behave similarly. This can be tested by means of a simple *t-test* on the standardized difference between $\bar{\theta}_b^*$ and $\bar{\theta}_a^*$

$$z_G = \frac{\bar{\theta}_a^* - \bar{\theta}_b^*}{\sqrt{\hat{V}(\bar{\theta}_a^*) + \hat{V}(\bar{\theta}_b^*)}} \sim N(0, 1).$$

We report the R statistics and p-values for the ergodic averages in [Figure C4](#). All the R statistics (blue bars) are below the 1.2 threshold, identified by the dotted blue line. Similarly, the red bars show that we do not reject the null hypothesis for any of the parameters.

D Score-driven framework

D.1 Score derivations

The scaled score s_t is a non-linear function of past observations and past parameters' values. For $\ell_t = \log \mathcal{D}(\theta, f_t)$ being the Skew-t of [Gómez et al. \(2007\)](#), $y_t|Y_{t-1} \sim Skt_\nu(\mu_t, \sigma_t^2, \varrho_t)$, the log-likelihood takes the form

$$\begin{aligned} \ell_t(r_t|\theta, \mathcal{F}_{t-1}) &= \log \mathcal{C}(\nu) - \frac{1}{2} \log \sigma_t^2 - \frac{1+\nu}{2} \log \left[1 + \frac{\varepsilon_t^2}{\nu(1 + \text{sgn}(\varepsilon_t)\varrho_t)^2 \sigma_t^2} \right], \\ \log \mathcal{C}(\nu) &= \log \Gamma\left(\frac{\nu+1}{2}\right) - \log \Gamma\left(\frac{\nu}{2}\right) - \frac{1}{2} \log \nu - \frac{1}{2} \log \pi, \end{aligned} \quad (\text{D1})$$

where $\Gamma(\cdot)$ is the Gamma function, $\text{sgn}(\cdot)$ is the sign function, and $\nu > 3$ are the degrees of freedom.

Differentiating [\(D1\)](#) with respect to location, scale and asymmetry we obtain the gradient vector

$\nabla_t = \left[\frac{\partial \ell_t}{\partial \mu}, \frac{\partial \ell_t}{\partial \sigma_t^2}, \frac{\partial \ell_t}{\partial \varrho_t} \right]'$. Recall that $\varepsilon_t = y_t - \mu_t$, $\zeta_t = \frac{\varepsilon_t}{\sigma_t}$ and let

$$f(\mu_t, \sigma_t^2, \varrho_t) = 1 + \frac{\varepsilon_t^2}{\nu(1 + \text{sgn}(\varepsilon_t)\varrho_t)^2 \sigma_t^2} = \frac{\nu(1 + \text{sgn}(\varepsilon_t)\varrho_t)^2 \sigma_t^2 + \varepsilon_t^2}{\nu(1 + \text{sgn}(\varepsilon_t)\varrho_t)^2 \sigma_t^2}$$

To avoid overburdening the notation, in what follows $\frac{\partial f(x)}{\partial x} = f'_x$ and $a = -\frac{1+\nu}{2}$. The score with respect to the location parameter reads

$$\frac{\partial \ell_t}{\partial \mu_t} = w_t \frac{\zeta_t}{\sigma_t}, \quad \text{with} \quad w_t = \frac{\nu + 1}{\nu (1 + \operatorname{sgn}(\varepsilon_t) \varrho_t)^2 + \zeta_t^2}.$$

Proof. Define

$$g(\mu_t) = a \log f(\mu_t, \sigma_t^2, \varrho_t),$$

such that $\frac{\partial \ell_t}{\partial \mu_t} = \frac{\partial g(\mu_t)}{\partial \mu_t} = a \frac{f'_{\mu_t}}{f(\mu_t, \sigma_t^2, \varrho_t)}$. For

$$f'_{\mu_t} = -\frac{2}{\nu(1 + \operatorname{sgn}(\varepsilon_t) \varrho_t)^2 \sigma_t^2} \varepsilon_t,$$

it follows:

$$\begin{aligned} \frac{\partial \ell_t}{\partial \mu_t} &= \frac{1 + \nu}{2} \frac{2}{\nu(1 + \operatorname{sgn}(\varepsilon_t) \varrho_t)^2 \sigma_t^2} \cdot \varepsilon_t \cdot \frac{\nu(1 + \operatorname{sgn}(\varepsilon_t) \varrho_t)^2 \sigma_t^2}{\nu(1 + \operatorname{sgn}(\varepsilon_t) \varrho_t)^2 \sigma_t^2 + \varepsilon_t^2} \\ &= \frac{(1 + \nu)}{\nu(1 + \operatorname{sgn}(\varepsilon_t) \varrho_t)^2 \sigma_t^2 + \varepsilon_t^2} \varepsilon_t \\ &= \omega_t \frac{\zeta_t}{\sigma_t} \end{aligned}$$

□

The score with respect to the squared scale parameter reads

$$\frac{\partial \ell_t}{\partial \sigma_t^2} = \frac{(w_t \zeta_t^2 - 1)}{2\sigma_t^2}.$$

Proof. Define

$$g(\sigma_t^2) = -\frac{\log \sigma_t^2}{2} + a \log f(\mu_t, \sigma_t^2, \varrho_t),$$

such that $\frac{\partial \ell_t}{\partial \sigma_t^2} = \frac{\partial g(\sigma_t^2)}{\partial \sigma_t^2} = -\frac{1}{2\sigma_t^2} + a \frac{f'_{\sigma_t^2}}{f(\mu_t, \sigma_t^2, \varrho_t)}$, with $f'_{\sigma_t^2} = -\frac{\varepsilon_t^2}{\nu(1+\text{sgn}(\varepsilon_t)\varrho_t)^2\sigma_t^4}$. It follows that:

$$\begin{aligned}\frac{\partial \ell_t}{\partial \sigma_t^2} &= -\frac{1}{2\sigma_t^2} - \frac{1+\nu}{2} \cdot \left[-\frac{\varepsilon_t^2}{\nu(1+\text{sgn}(\varepsilon_t)\varrho_t)^2\sigma_t^4} \cdot \frac{\nu(1+\text{sgn}(\varepsilon_t)\varrho_t)^2\sigma_t^2}{\nu(1+\text{sgn}(\varepsilon_t)\varrho_t)^2\sigma_t^2 + \varepsilon_t^2} \right] \\ &= -\frac{1}{2\sigma_t^2} - \frac{1+\nu}{2} \cdot \left[-\frac{\varepsilon_t^2}{\sigma_t^2} \cdot \frac{1}{\nu(1+\text{sgn}(\varepsilon_t)\varrho_t)^2\sigma_t^2 + \varepsilon_t^2} \right] \\ &= -\frac{1}{2\sigma_t^2} + \frac{w_t\zeta_t^2}{2\sigma_t^2} = \frac{(w_t\zeta_t^2 - 1)}{2\sigma_t^2}\end{aligned}$$

□

The score with respect to the shape parameter reads as

$$\frac{\partial \ell_t}{\partial \varrho_t} = \frac{\text{sgn}(\varepsilon_t)}{(1 + \text{sgn}(\varepsilon_t)\varrho_t)} w_t \zeta_t^2.$$

Proof. Define

$$g(\varrho_t) = a \log f(\mu_t, \sigma_t^2, \varrho_t),$$

such that $\frac{\partial \ell_t}{\partial \varrho_t} = \frac{\partial g(\varrho_t)}{\partial \varrho_t} = a \frac{f'_{\varrho_t}}{f(\mu_t, \sigma_t^2, \varrho_t)}$, with $f'_{\varrho_t} = -\frac{2(\text{sgn}(\varepsilon_t) + \varrho_t)\varepsilon_t^2}{\nu(1+\text{sgn}(\varepsilon_t)\varrho_t)^4\sigma_t^2}$. It follows that:

$$\begin{aligned}\frac{\partial \ell_t}{\partial \varrho_t} &= \frac{1+\nu}{2} \cdot \frac{2(\text{sgn}(\varepsilon_t) + \varrho_t)\varepsilon_t^2}{\nu(1+\text{sgn}(\varepsilon_t)\varrho_t)^4\sigma_t^2} \cdot \frac{\nu(1+\text{sgn}(\varepsilon_t)\varrho_t)^2\sigma_t^2}{\nu(1+\text{sgn}(\varepsilon_t)\varrho_t)^2\sigma_t^2 + \varepsilon_t^2} \\ &= \frac{(\text{sgn}(\varepsilon_t) + \varrho_t)\varepsilon_t^2 w_t}{(1 + \text{sgn}(\varepsilon_t)\varrho_t)^2 \sigma_t^2} = \frac{\text{sgn}(\varepsilon_t)}{(1 + \text{sgn}(\varepsilon_t)\varrho_t)} w_t \zeta_t^2\end{aligned}$$

□

D.2 Scaled scores

Given we model $\gamma_t = \log \sigma_t$ and $\delta_t = \text{atanh}(\varrho_t)$, for the chain rule we have:

$$\frac{\partial \ell_t}{\partial \gamma_t} = \frac{\partial \ell_t}{\partial \sigma_t^2} \frac{\partial \sigma_t^2}{\partial \gamma_t}, \quad \frac{\partial \ell_t}{\partial \delta_t} = \frac{\partial \ell_t}{\partial \varrho_t} \frac{\partial \varrho_t}{\partial \delta_t}, \quad (\text{D2})$$

where $\frac{\partial \sigma_t^2}{\partial \gamma_t} = 2\sigma_t^2$ and $\frac{\partial \varrho_t}{\partial \delta_t} = (1 - \varrho_t^2)$. We can thus define the vector of interest as $f_t = (\mu_t, \gamma_t, \delta_t)'$ with the associated Jacobian matrix

$$J_t = \frac{\partial(\mu_t, \sigma_t^2, \varrho_t)}{\partial f_t'} = \begin{bmatrix} 1 & 0 & 0 \\ 0 & 2\sigma_t^2 & 0 \\ 0 & 0 & 1 - \varrho_t^2 \end{bmatrix}. \quad (\text{D3})$$

The Fisher information matrix is computed as the expected value of outer product of the gradient vector. Given the degrees of freedom $\nu > 3$ this is computed as:

$$\mathcal{I}_t = \mathbb{E}_{t-1}[\nabla_t \nabla_t'] = \begin{bmatrix} \frac{(1+\nu)}{(\nu+3)(1-\varrho_t^2)\sigma_t^2} & 0 & \frac{4(1+\nu)}{\sigma_t(1-\varrho_t^2)(3+\nu)} \\ 0 & \frac{1}{2(3+\nu)\sigma_t^4} & 0 \\ \frac{4(1+\nu)}{\sigma_t(1-\varrho_t^2)(3+\nu)} & 0 & \frac{3(1+\nu)}{(1-\varrho_t^2)(3+\nu)} \end{bmatrix}. \quad (\text{D4})$$

As a result, the vector of scaled scores reads as:

$$\mathbf{s}_t = (J_t' \text{diag}(\mathcal{I}_t) J_t)^{-\frac{1}{2}} J_t' \nabla_t = \begin{bmatrix} s_{\mu,t} \\ s_{\gamma,t} \\ s_{\delta,t} \end{bmatrix} = \begin{bmatrix} \sqrt{\frac{(\nu+3)(1-\varrho_t^2)}{(\nu+1)}} w_t \zeta_t \\ \sqrt{\frac{(\nu+3)}{2\nu}} (w_t \zeta_t^2 - 1) \\ \text{sgn}(\varepsilon_t) \sqrt{\frac{(\nu+3)(1-\text{sgn}(\varepsilon_t)\varrho_t)}{3(\nu+1)(1+\text{sgn}(\varepsilon_t)\varrho_t)}} w_t \zeta_t^2 \end{bmatrix}. \quad (\text{D5})$$

Full derivations for the Information matrix are provided in [Delle Monache et al. \(2024\)](#).

E Monte Carlo analysis

We simulate $T=250$ observations from $Skt_\nu(\mu_t, \sigma_t, \varrho_t)$, for simulated values of the parameters of location, μ_t , scale, σ_t , and asymmetry, ϱ_t . Unless explicitly mentioned, we simulate the parameters independently, and we consider the following cases: no asymmetry, breaks in the asymmetry, fixed asymmetry with location-scale covariance, fixed asymmetry with location-scale covariance with breaks, time-varying asymmetry, and time-varying asymmetry with breaks in the location-scale covariance.

For all cases, we simulate the location and log-scale from first order Gaussian autoregressive

processes, with autoregressive parameters equal to 0.9 and 0.99, respectively, and variances set to 0.05 and 0.025. When we assume correlated innovations for the two parameters, we set this to 0.4. When we impose breaks in this correlation, we assume the relation abruptly shifts to 0.8 after 100 observations, and then falls to -0.4 after additional 50 observations. When time-varying, the asymmetry parameter is simulated from an AR(1) with persistence set to 0.9 and variance 0.025; when only breaks are considered, these occur on the 100th observation, moving from 0 to 0.25, and a sharp fall to -0.25 on the 150th observation.

Define $\delta_t = \log \sigma_t$, $\varrho_t = \text{arctanh } \varrho_t$, and $\varepsilon \sim \mathcal{N}(0, 1)$, and let $\text{chol}()$ define the lower-triangular Choleski factor; here we report a summary of the six DGPs.

DGP1: no asymmetry

$$\begin{bmatrix} \mu_t \\ \delta_t \end{bmatrix} = \begin{bmatrix} 0.9 & 0 \\ 0 & 0.99 \end{bmatrix} \begin{bmatrix} \mu_{t-1} \\ \delta_{t-1} \end{bmatrix} + \text{chol} \left(\begin{bmatrix} 0.05 & 0 \\ 0 & 0.025 \end{bmatrix} \right) \varepsilon_t,$$

$$\gamma_t = 0, \forall t$$

DGP2: constant asymmetry with breaks

$$\begin{bmatrix} \mu_t \\ \delta_t \end{bmatrix} = \begin{bmatrix} 0.9 & 0 \\ 0 & 0.99 \end{bmatrix} \begin{bmatrix} \mu_{t-1} \\ \delta_{t-1} \end{bmatrix} + \text{chol} \left(\begin{bmatrix} 0.05 & 0 \\ 0 & 0.025 \end{bmatrix} \right) \varepsilon_t,$$

$$\gamma_t = \begin{cases} 0 & t \leq 100 \\ 0.25 & 100 < t \leq 150 \\ -0.25 & t < 150 \end{cases}$$

DGP3: no asymmetry and location-scale covariance

$$\begin{bmatrix} \mu_t \\ \delta_t \end{bmatrix} = \begin{bmatrix} 0.9 & 0 \\ 0 & 0.99 \end{bmatrix} \begin{bmatrix} \mu_{t-1} \\ \delta_{t-1} \end{bmatrix} + chol \left(\begin{bmatrix} 0.05 & 0 \\ 0 & 0.025 \end{bmatrix}^{\frac{1}{2}} \begin{bmatrix} 1 & .4 \\ .4 & 1 \end{bmatrix} \begin{bmatrix} 0.05 & 0 \\ 0 & 0.025 \end{bmatrix}^{\frac{1}{2}} \right) \varepsilon_t,$$

$$\gamma_t = 0 \forall t$$

DGP4: no asymmetry and location-scale covariance with breaks

$$\begin{bmatrix} \mu_t \\ \delta_t \end{bmatrix} = \begin{bmatrix} 0.9 & 0 \\ 0 & 0.99 \end{bmatrix} \begin{bmatrix} \mu_{t-1} \\ \delta_{t-1} \end{bmatrix} + chol \left(\begin{bmatrix} 0.05 & 0 \\ 0 & 0.025 \end{bmatrix}^{\frac{1}{2}} \begin{bmatrix} 1 & \rho_t \\ \rho_t & 1 \end{bmatrix} \begin{bmatrix} 0.05 & 0 \\ 0 & 0.025 \end{bmatrix}^{\frac{1}{2}} \right) \varepsilon_t,$$

$$\rho_t = \begin{cases} 0.4 & t \leq 100 \\ 0.8 & 100 < t \leq 150, \\ -0.4 & t > 150 \end{cases}$$

$$\gamma_t = 0 \forall t$$

DGP5: time-varying asymmetry

$$\begin{bmatrix} \mu_t \\ \delta_t \\ \gamma_t \end{bmatrix} = \begin{bmatrix} 0.9 & 0 & 0 \\ 0 & 0.99 & 0 \\ 0 & 0 & 0.9 \end{bmatrix} \begin{bmatrix} \mu_{t-1} \\ \delta_{t-1} \\ \gamma_{t-1} \end{bmatrix} + chol \left(\begin{bmatrix} 0.05 & 0 & 0 \\ 0 & 0.025 & 0 \\ 0 & 0 & 0.025 \end{bmatrix} \right) \varepsilon_t$$

DGP5: time-varying asymmetry and correlated updates

$$\begin{bmatrix} \mu_t \\ \delta_t \\ \gamma_t \end{bmatrix} = \begin{bmatrix} 0.9 & 0 & 0 \\ 0 & 0.99 & 0 \\ 0 & 0 & 0.9 \end{bmatrix} \begin{bmatrix} \mu_{t-1} \\ \delta_{t-1} \\ \gamma_{t-1} \end{bmatrix} + chol \left(\begin{bmatrix} 0.05 & 0 \\ 0 & 0.025 \end{bmatrix}^{\frac{1}{2}} \begin{bmatrix} 1 & \rho_t & 0.2 \\ \rho_t & 1 & 0.3 \\ 0.2 & 0.3 & 1 \end{bmatrix} \begin{bmatrix} 0.05 & 0 \\ 0 & 0.025 \end{bmatrix}^{\frac{1}{2}} \right) \varepsilon_t,$$

$$\rho_t = \begin{cases} 0.4 & t \leq 100 \\ 0.8 & 100 < t \leq 150 \\ -0.4 & t > 150 \end{cases}$$

We report the results of this exercise in [Figure E1](#). Specifically, for DGP1 to DGP4 we report in blue the estimated asymmetry, with 68% and 90% credible sets represented by shades of gray, against the simulated parameter, in red. For DGP5 and DGP6 we report the distribution of the difference between the estimated and the simulated asymmetry.

For the first DGP, data are simulated under the assumption of symmetry, with independent, time-varying location and volatility. We show that the model does not pick up any asymmetry when this is not a feature of the data. The second DGP considers the case in which the asymmetry parameter experiences a break from 0 to 0.25 after 100 observations, hence implying positively skewed distributions, and another jump to -0.25 after additional 50 observations; this second jump changes the sign of the skewness. Three comments are in order. First, as for DGP1, no asymmetry is detected when the true value is zero. Second, the parameter reacts promptly to the first jump, despite only 50 observations feature positive skewness. Third, the model quickly detects a turning point in the sign of the asymmetry, turning from positive to negative in less than 20 periods.

DGP3 and DGP4 are meant to provide reassurances that the model does not mistake correlations between the location and the scale for evidence of asymmetry. In DGP4 we further allow for the correlation to experience breaks, that flip the sign of the covariance between the two parameters. The reported results highlight that the model provides asymmetry estimates that are robust to such features of the data.

Finally, in DGP5 and DGP6 we simulate the asymmetry parameter to vary over time, as the other two parameters. The two DGPs differ in the covariance structure of the parameters: DGP5 assumes independent innovations to the processes, whereas DGP6 assumes a full covariance matrix, with the covariance between location and scale experiencing two breaks, as in DGP4. Once again, we document that our model is successful in detecting the correct sign and dynamics for the asymmetry parameter, even when all the parameters are correlated, and experience instability.

Returning to DGP2, we evaluate the ability of the model to distinguish permanent changes in the parameter against transitory moves. [Figure E2](#) report the estimated long- and short-run components; notice that the two distributions add up to that reported in panel (b) of [Figure E1](#). The model successfully discerns the persistence of the asymmetry in the data whereby it correctly picks up permanent changes. Interestingly, the short-run component shows short periods of increased volatility around the observations where the DGP jumps. This suggests that at first the model interprets new observations as transitory changes in the data, but as more evidence comes through, the long-run component quickly learns the new feature of the data, whereas the short-term component reverts to zero.

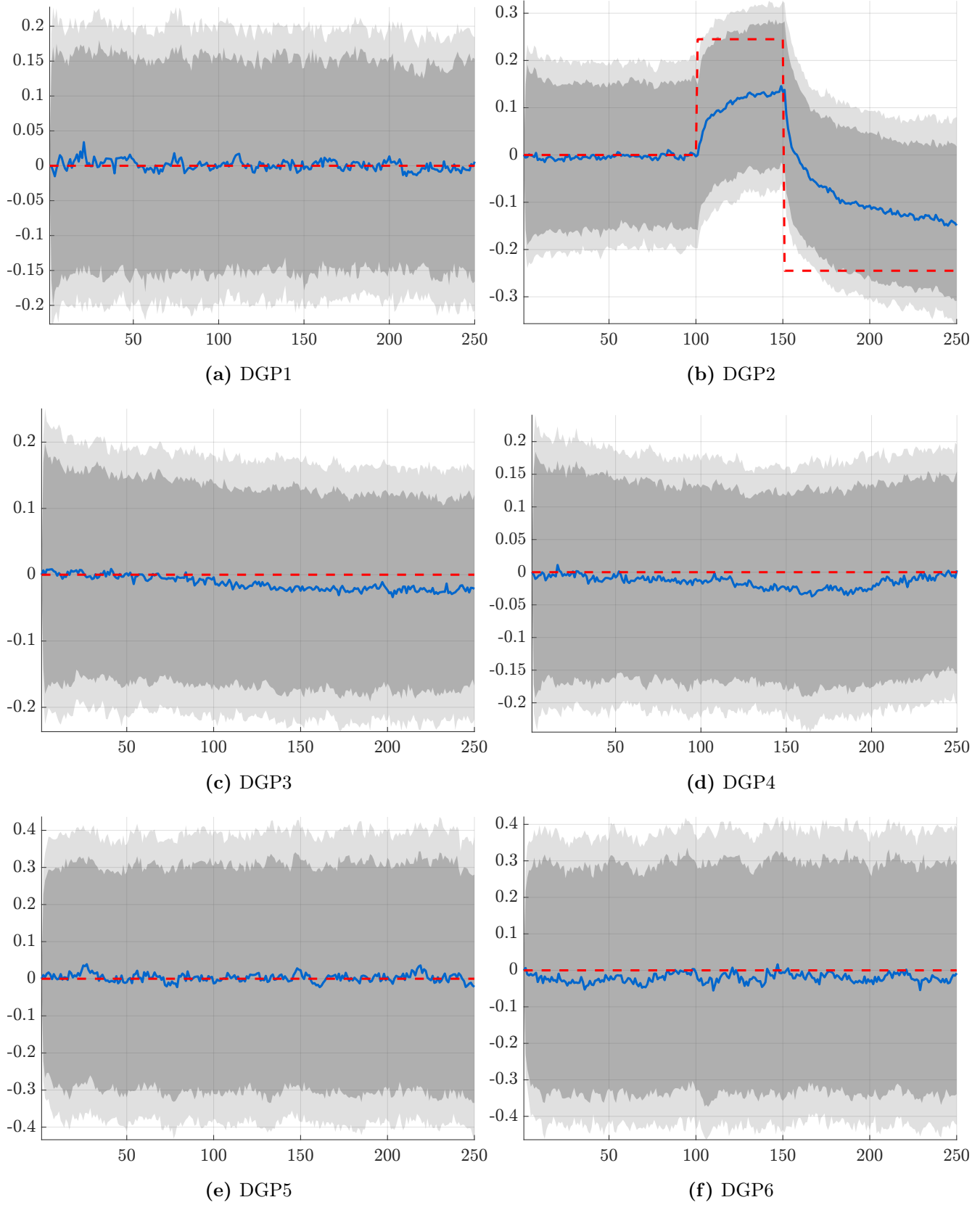


Figure E1: Estimated asymmetry

Note: The panels reports the estimated paths for the asymmetry parameters (blue) with the associated 68% and 90% credible sets. The asymmetry under the DGP is reported in red. For DGP 5 and 6 we report deviations of the estimated parameter from the simulated values. We consider $T=250$ observations for 1000 Monte Carlo replications.

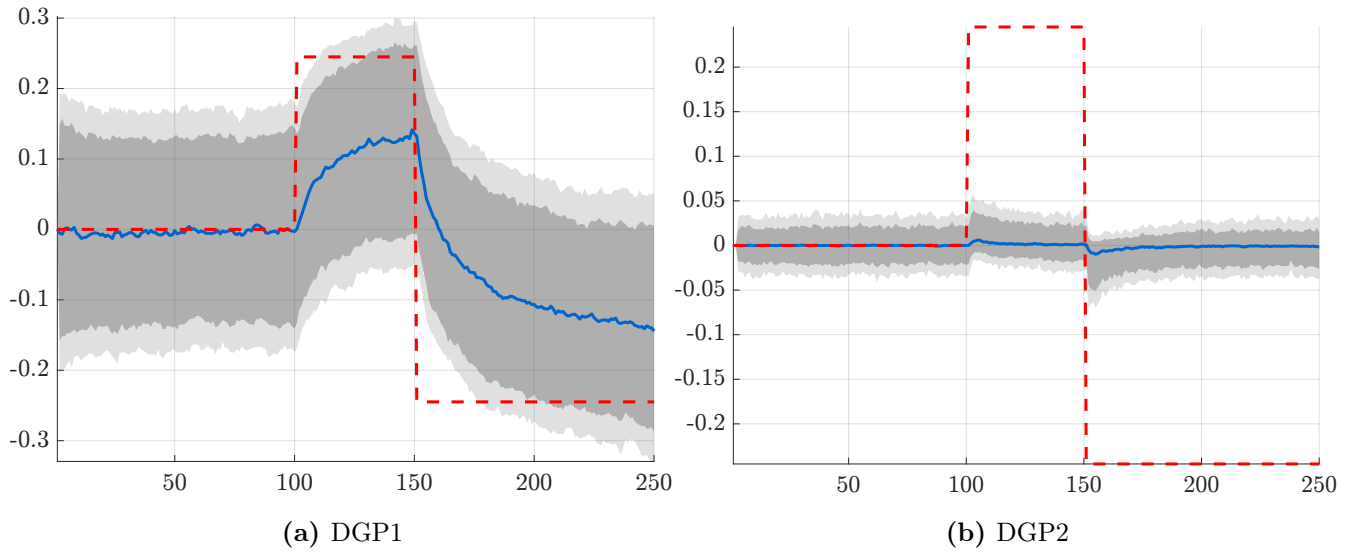


Figure E2: Disentangling permanent changes

Note: The panel report the estimates long- (a) and short- (b) components of the asymmetry parameters estimated under DGP2. Median values are reported in blue, with the associated 68% and 90% credible sets in gray. The asymmetry under the DGP is reported in red. We consider $T=250$ observations for 1000 Monte Carlo replications.

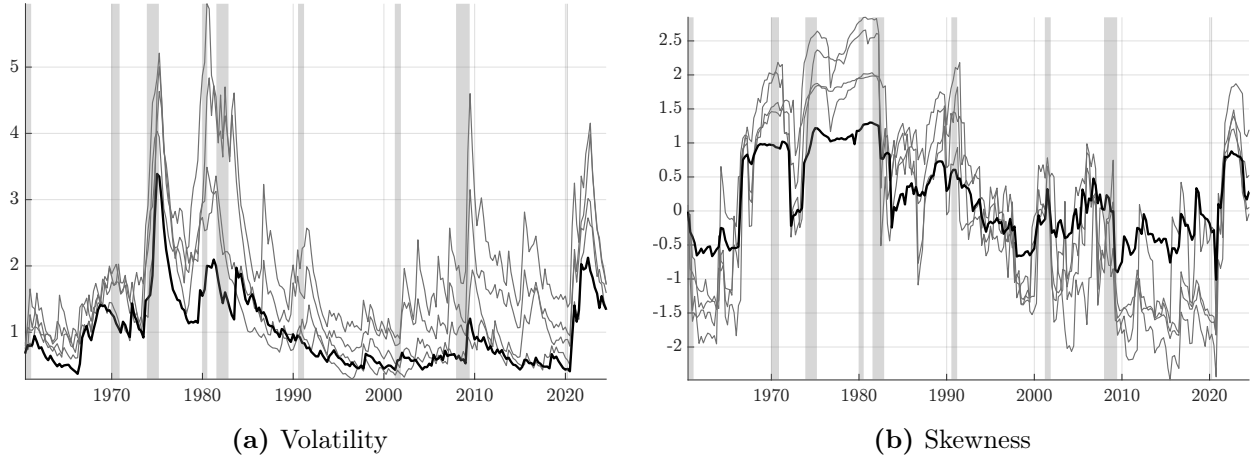


Figure F1: Risk across different inflation measures

Note: The panels report the full moment median estimates volatilities (a) and skewness (b) for different measures of inflation. Black lines indicate estimates for core PCE. Other inflation measures we consider are: GDP deflator, headline PCE, headline CPI and core CPI. Gray shaded areas represent NBER recessions.

F Evidence of time variation in inflation risk for other inflation measures

In this appendix we report additional results about the time variation in the risks of policy relevant measures of inflation. Within the framework introduced in [Section 4](#), we can formally test the null hypothesis that ϱ_t remains constant over the entire sample. [Table F1](#) presents the results of three parametric Lagrange Multiplier tests: the Q test, the adjusted Q* test, and the Nyblom test as outlined by [Delle Monache et al. \(2024\)](#). These tests differ in their chosen alternative hypotheses, resulting in varying statistical power (see, e.g., [Harvey, 2013](#)). We consider two scenarios: one assuming constant volatility over time and another allowing for time-varying volatility. In both cases, the tests strongly reject the null hypothesis of symmetry at the 1% confidence level.

[Table F1](#) collect the test statistics for the detection of time variation in the asymmetry for all four measures of inflation. Overall, the null of restricted asymmetry is strongly rejected.

We also conduct additional tests using rolling estimates of inflation asymmetry. These tests further underscore the importance of accounting for time-varying skewness when tracking the conditional distribution of inflation (see [Appendix C](#)).

[Figure F1](#) shows the estimated dynamics of inflation volatility and skewness across the different measures, highlighting in black that of core PCE. Two comments are in order. First, the dynamics

Table F1: Time variation in higher order moments

	Q	Q^*	N	Q	Q^*	N
	GDP Deflator			Headline PCE		
	<i>Homoskedastic</i>					
<i>Shape</i>	637.470***	644.910***	5.690***	303.820***	307.370***	6.460***
	<i>Heteroskedastic</i>					
<i>Scale</i> ²	597.120***	604.090***	4.050***	566.190***	572.800***	2.330***
<i>Shape</i>	154.150***	155.950***	2.780***	148.610***	150.350***	1.890***
	Core CPI			Headline CPI		
	<i>Homoskedastic</i>					
<i>Shape</i>	840.710***	850.480***	3.290***	407.600***	412.340***	4.220***
	<i>Heteroskedastic</i>					
<i>Scale</i> ²	556.980***	563.460***	3.810***	730.210***	738.700***	3.430***
<i>Shape</i>	185.210***	187.360***	3.260***	183.040***	185.160***	2.150***

Note: Q is the portmanteau test, Q^* is the Ljung-Box extension (with automatic lag selection) and N corresponds to the Nyblom test. Q and Q^* are distributed as a χ^2_1 , while N is distributed as a Cramer von-Mises distribution with 1 degree of freedom. * $p < 10\%$, ** $p < 5\%$, *** $p < 1\%$.

of the two moments is extremely similar for all measures. With varying magnitudes, volatilities spike around recessions, and remain persistently high soon after. Skewness follow humped-shape patterns in the 1970s and 1980s, then moving downward since the 1990s, remaining negative until the pandemic period. Second, it's important to note that, among all these measures, core PCE shows the least variation in both volatility and skewness, appearing to be the more stable measure of price dynamics. Based on previous results, we also report the estimates for the time-varying moments of the four measures.

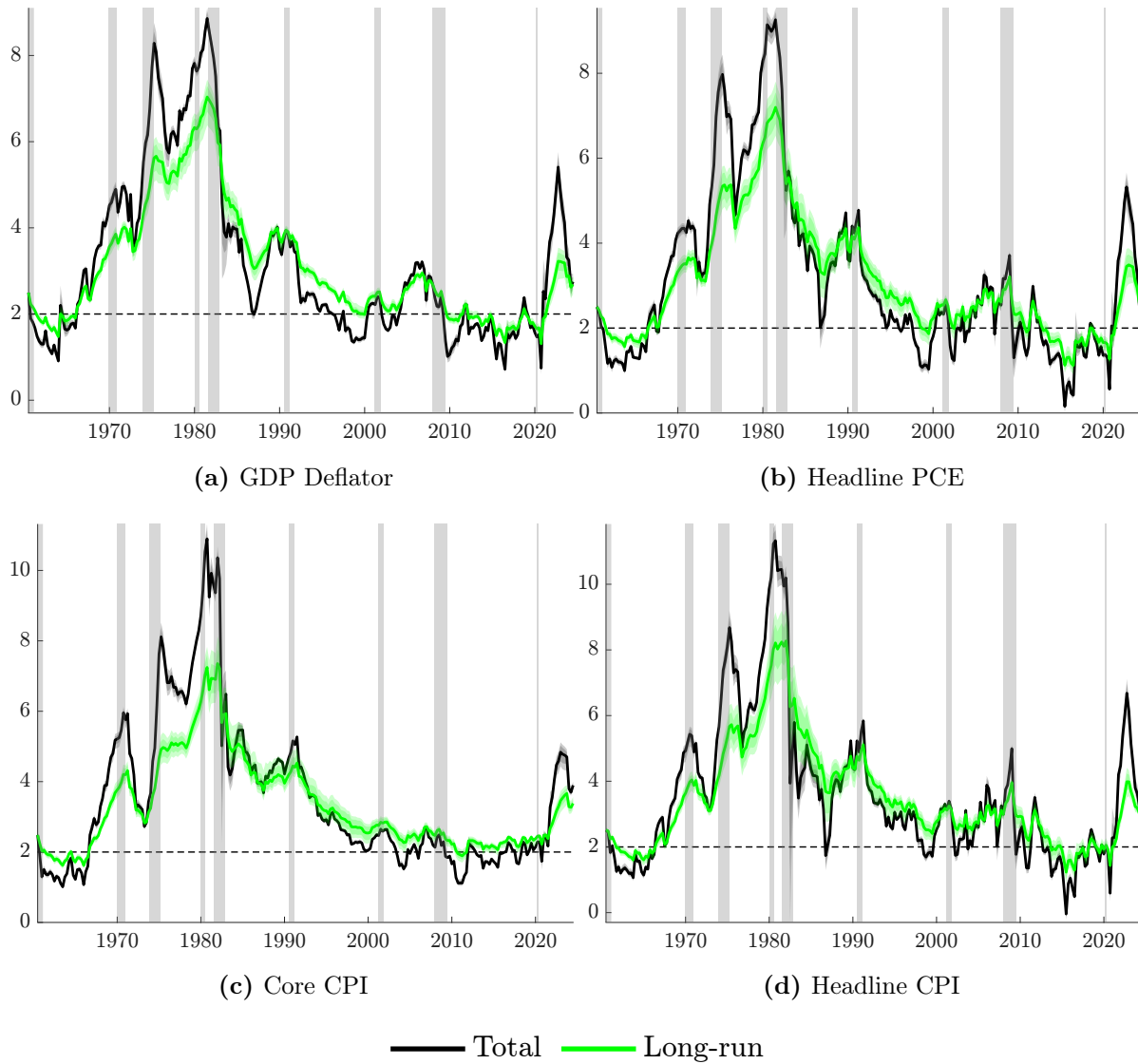


Figure F2: Estimated mean for different inflation measures

Note: The panels report the estimated total (black) and long-run (green) mean for: (a) GDP deflator, (b) headline PCE, (c) core CPI, and (d) headline CPI. ray shaded areas represent NBER recessions.

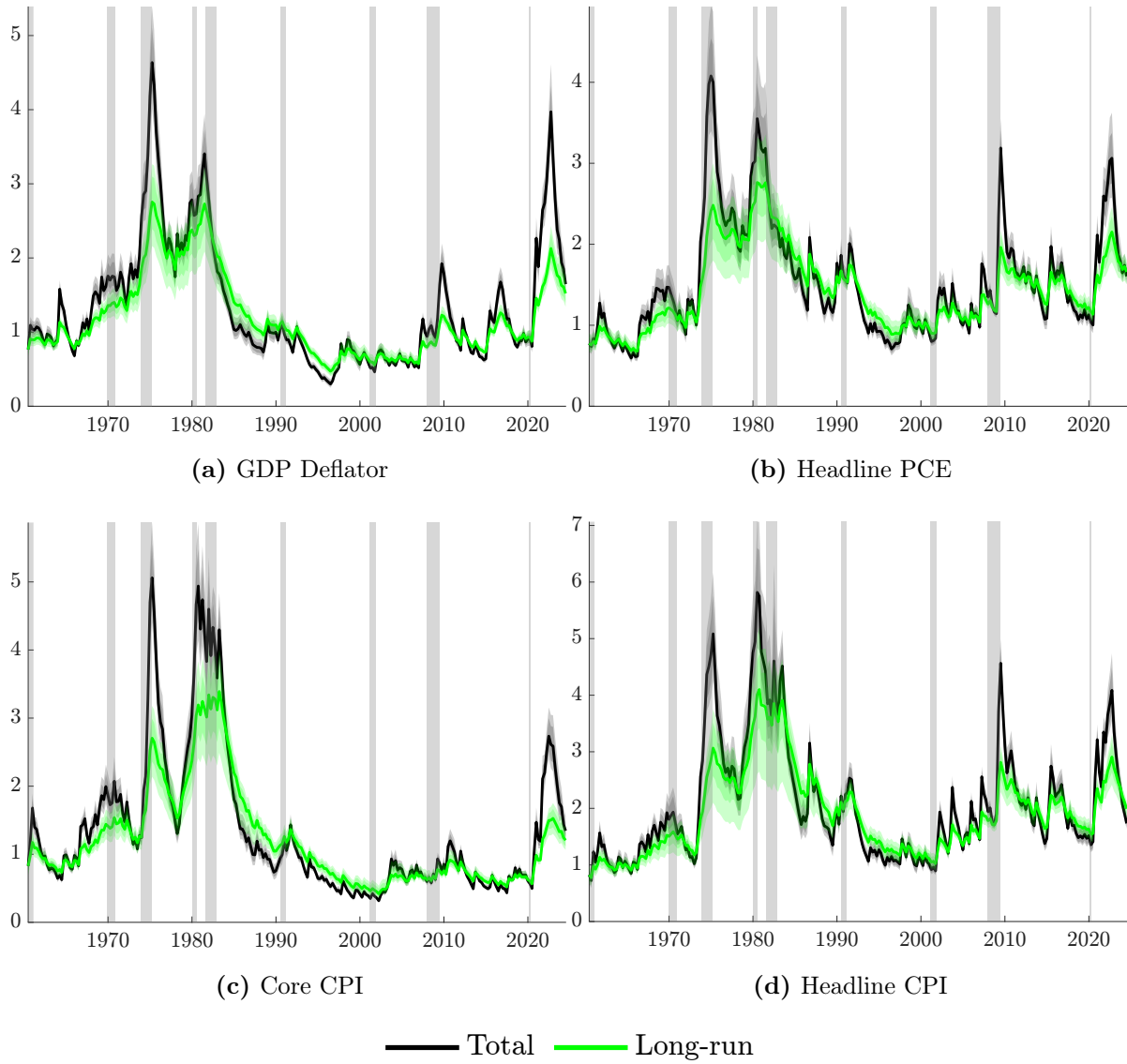


Figure F3: Estimated volatility for different inflation measures

Note: The panels report the estimated total (black) and long-run (green) volatility for: (a) GDP deflator, (b) headline PCE, (c) core CPI, and (d) headline CPI. ray shaded areas represent NBER recessions.

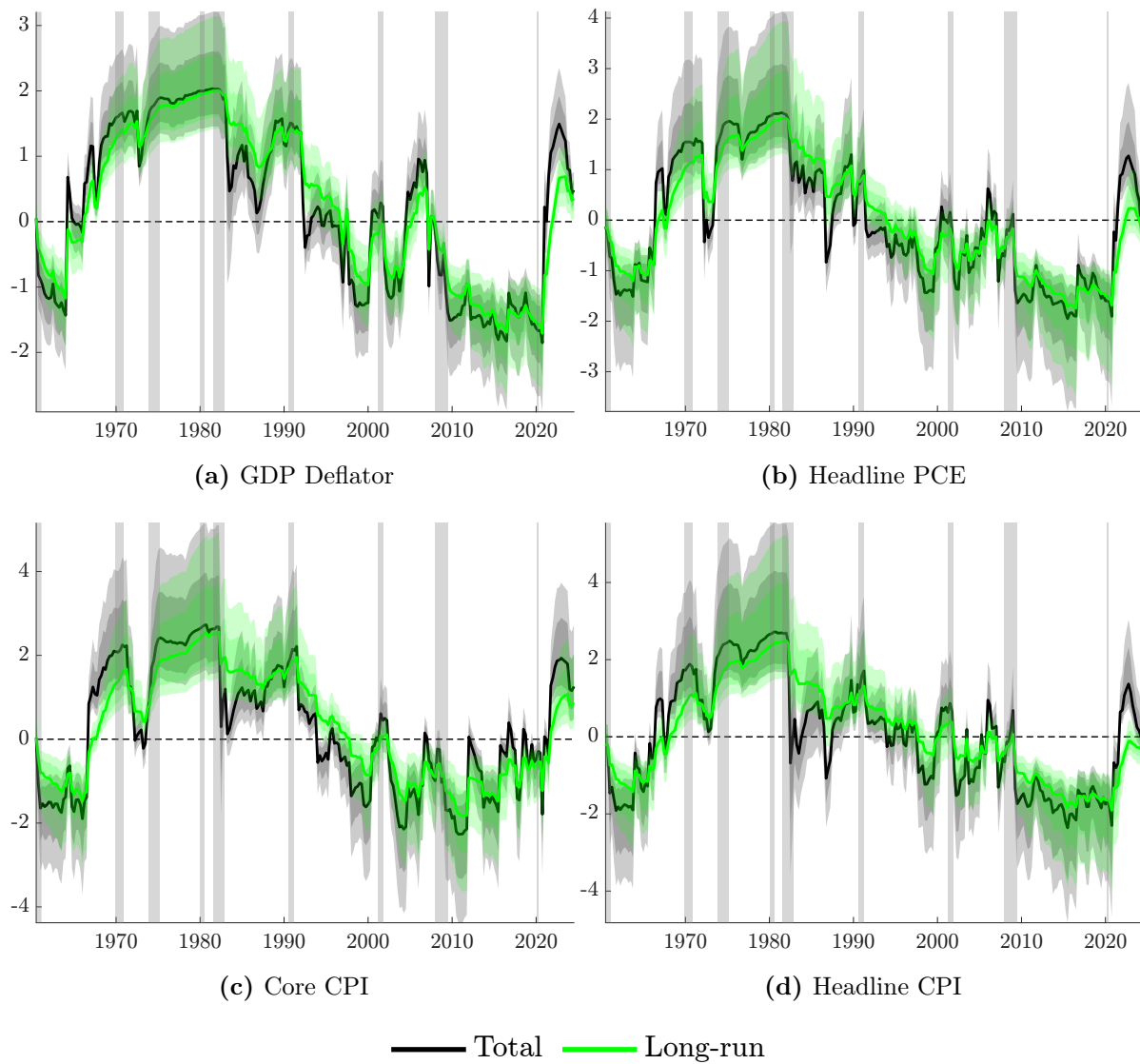


Figure F4: Estimated skewness for different inflation measures

Note: The panels report the estimated total (black) and long-run (green) skewness for: (a) GDP deflator, (b) headline PCE, (c) core CPI, and (d) headline CPI. ray shaded areas represent NBER recessions.

G RAIT vs FAIT: implicit inflation target

In this section, we compare practical implementations of the Flexible Average Inflation Targeting (FAIT) with our Risk-Adjusted Inflation Targeting (RAIT) strategy. Under FAIT, the central bank determines its temporary inflation overshoot by considering past deviations from the 2% statutory inflation target. This target can be written as

$$\pi_t^{\text{FAIT}} = \hat{\pi}_t^{\text{FAIT}} + \bar{\pi} \quad \text{where} \quad \hat{\pi}_t^{\text{FAIT}} = \rho_F \hat{\pi}_{t-1}^{\text{FAIT}} - (1 - \rho_F) [\pi_t^{\text{Data}} - \bar{\pi}],$$

and $\bar{\pi}$ is the 2% target. The expression in brackets captures current inflation misses, while $\rho_F \in (0, 1)$ controls how quickly the central bank corrects past deviations. Lower ρ_F implies short memory and higher target variability; higher ρ_F results in a smoother, slower-moving target.

Figure G1 illustrates the FAIT-implied target for different ρ_F values—e.g., 0.95, 0.9, and 0.8—corresponding to look-back horizons with half-life of 3, 1.5 and 0.75 years. Over the 2010–2020 period, when inflation consistently ran below target, FAIT would have implied a persistent overshoot of 40 to 60 basis points. In contrast, RAIT calls for only a modest overshoot of roughly 15 basis points during 2009–2011, after which the RAIT target returns to the statutory 2%. These differences reflect the quantitative relevance of skewed risks during each period. Recalling that the bias associated with skewed risk can be expressed as $\psi_{t+h} = g(\nu)\sigma_{t+h}\varrho_{t+h}$, we note that although risks were predominantly skewed to the downside after 2009, the low inflation volatility during that period limited their impact on the overall balance of risks.²⁹ Notably, the RAIT target begins rising ahead of the FAIT target, consistent with its forward-looking design.

Zooming into the 2021 inflation surge, FAIT’s implicit target lags behind RAIT’s, making policy less proactive. FAIT’s backward-looking nature limits its responsiveness to changing inflation dynamics. When risks shifted rapidly, FAIT was slower than RAIT in signaling the need for a policy adjustment. This delay likely contributed to the Fed’s late tightening in 2021–2022. By the end of the sample, FAIT also fails to capture the rapid normalization of inflation risks. As inflation peaks following persistent overshoots, FAIT would require implausibly low targets

²⁹Inflation volatility spiked during the Great Recession but remained low throughout the following decade, before rising again after 2020.

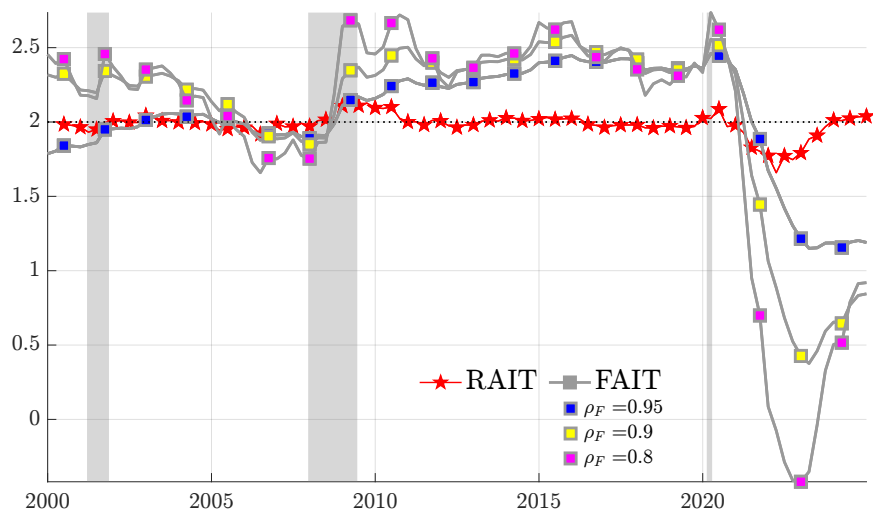


Figure G1: RAIT vs FAIT: Inflation Target

Note: The figure displays the RAIT inflation target, which reflects the central bank’s commitment to offset perceived future (unbalanced) risks, alongside the evolving inflation target under FAIT, where deviations from 2% are intended to compensate for past misses of the target.

to correct earlier misses. In contrast, RAIT’s flexibility would have allowed the central bank to recognize the improving outlook and justify monetary easing as early as early 2023—a shift identified in real time by the model in [Section 4](#).

References

- ARELLANO-VALLE, R. B., H. W. GÓMEZ, AND F. A. QUINTANA (2005): “Statistical inference for a general class of asymmetric distributions,” *Journal of Statistical Planning and Inference*, 128, 427–443.
- BAI, J. AND S. NG (2005): “Tests for skewness, kurtosis, and normality for time series data,” *Journal of Business & Economic Statistics*, 23, 49–60.
- BLASQUES, F., J. VAN BRUMMELEN, S. J. KOOPMAN, AND A. LUCAS (2022): “Maximum likelihood estimation for score-driven models,” *Journal of Econometrics*, 227, 325–346.
- CHAHROUR, R. AND K. JURADO (2018): “News or Noise? The Missing Link,” *American Economic Review*, 108, 1702–36.
- COGLEY, T. AND T. J. SARGENT (2005): “Drifts and volatilities: monetary policies and outcomes in the post WWII US,” *Review of Economic Dynamics*, 8, 262–302.
- CREAL, D., S. J. KOOPMAN, AND A. LUCAS (2013): “Generalized autoregressive score models with applications,” *Journal of Applied Econometrics*, 28, 777–795.
- DE POLIS, A. (2023): “Conditional asymmetries and downside risks in macroeconomic and financial time series,” Ph.D. thesis, University of Warwick.
- DELLE MONACHE, D., A. DE POLIS, AND I. PETRELLA (2024): “Modeling and forecasting macroeconomic downside risk,” *Journal of Business & Economic Statistics*, 42, 1010–1025.
- DOAN, T., R. LITTERMAN, AND C. SIMS (1984): “Forecasting and conditional projection using realistic prior distributions,” *Econometric Reviews*, 3, 1–100.
- GALÍ, J. (2008): *Monetary Policy, Inflation, and the Business Cycle: An Introduction to the New Keynesian Framework*, Princeton University Press.
- GELMAN, A. (1995): “Inference and monitoring,” *Markov chain Monte Carlo in practice*, 131.
- GELMAN, A. AND D. B. RUBIN (1992): “Inference from iterative simulation using multiple sequences,” *Statistical science*, 7, 457–472.
- GEWEKE, J. (1992): “Evaluating the Accuracy of Sampling-Based Approaches to the Calculation of Posterior Moments,” in *Bayesian Statistics 4: Proceedings of the Fourth Valencia International Meeting, Dedicated to the memory of Morris H. DeGroot, 1931–1989*, Oxford University Press.
- GÓMEZ, H. W., F. J. TORRES, AND H. BOLFARINE (2007): “Large-sample inference for the epsilon-skew-t distribution,” *Communications in Statistics—Theory and Methods*, 36, 73–81.
- HAARIO, H., E. SAKSMAN, AND J. TAMMINEN (1999): “Adaptive proposal distribution for random walk Metropolis algorithm,” *Computational Statistics*, 14, 375–396.
- HARVEY, A. AND S. THIELE (2016): “Testing against changing correlation,” *Journal of Empirical Finance*, 38, 575–589.
- HARVEY, A. C. (2013): *Dynamic models for volatility and heavy tails: with applications to financial and economic time series*, vol. 52, Cambridge University Press.

- SHERLOCK, C., A. GOLIGHTLY, AND D. A. HENDERSON (2017): “Adaptive, delayed-acceptance MCMC for targets with expensive likelihoods,” *Journal of Computational and Graphical Statistics*, 26, 434–444.
- SIMS, C. (2002): “Solving Linear Rational Expectations Models,” *Computational Economics*, 20, 1–20.
- SIMS, C. A. AND T. ZHA (1998): “Bayesian methods for dynamic multivariate models,” *International Economic Review*, 949–968.